CONTROLLED WET-CHEMICAL DISSOLUTION OF SIMULATED HIGH-TEMPERATURE REACTOR COATED FUEL PARTICLES

by

Kholiswa Patricia Skolo

29686378

Submitted in partial fulfilment of the requirements for the degree

MSc (Applied Science)

In the Department of Chemical Engineering

Faculty of Engineering, Built Environment & Information Technology

University of Pretoria

Republic of South Africa

Supervisor: Prof. P.L. Crouse

July 2012

DECLARATION

I declare that this dissertation "C*ontrolled wet-chemical dissolution of simulated high-temperature reactor coated fuel particles"* is my own work and has not been submitted before for any degree or examination in any other university, and that all the sources I have used or quoted have been indicated and acknowledged as complete references.

Kholiswa Patricia Skolo

Signature: ..... Date: .....

ACKNOWLEDGEMENTS

I wish to extend my sincere gratitude to the following people without whose support and guidance this study would have been difficult:

My creator and Father in heaven, the almighty God, I thank him for giving me the ability, strength and wisdom to complete this work.

My supervisor Professor Philip Crouse for his guidance, support and encouragement during this study. Thank you for being patient with me.

I would like to extend my appreciation to the Hot Cell Projects Group of the South African Nuclear Energy Corporation (Necsa) for their support and guidance. My deepest gratitude goes to Mr. Wouter Klopper, my manager, for inspiring me to pursue this study. The continuous moral support you demonstrated throughout this study is much appreciated; you were an inspiration. Without you, this journey would have been difficult. Dr John Barry you helped me to improve my knowledge of TRISO particles, thank you for availing yourself.

I gratefully acknowledge the support of Mr. André Botha of the University of Pretoria Laboratory for Microscopy and Microanalysis with SEM studies.

Thank you Dr Johan Venter, Dr Oosthuizen and Trudy Jacobs for editing parts of this work.

Sincere thanks to my family and friends for your encouragement and support. Sinobomi and Bongani thank you for your prayers, love and support. To my grandmother ndiyabulela Ngwevu ngemfundiso zakho.

I also wish to express my gratitude to Necsa and NRF for financial support as well as the Applied Chemistry Division at Necsa for allowing the use of their laboratories.

ABSTRACT

High-temperature reactors make use of tri-structural coated fuel particles as basic fuel components. These TRISO particles consist of fissionable uranium dioxide fuel kernels, about 0.5 mm in diameter, with each kernel individually encased in four distinct coating layers, starting with a porous carbon buffer, then an inner pyrolytic carbon (IPyC) layer, followed by a layer of ceramic silicon carbide (SiC) and finally an outer pyrolytic carbon layer (OPyC). Collectively, the coating layers provide the primary barrier that prevents release of fission products generated during burn up in the UO_2 fuel kernel. It is crucial to understand how the fission products contained within the fuel interact with the coating layers and how they are distributed within the fuel. The first step commonly performed to obtain the information on distribution is removal of the coating layers.

The purpose of this study was to investigate the possible use of wet chemical etching techniques with the aim of removing the coating layers of ZrO_2 coated fuel particles in a controlled way and to establish experimental parameters for controlled dissolution of irradiated fuel particles.

Stepwise dissolution of coated fuel particle coating layers, containing zirconia kernels has been investigated by chemical etching experiments with acidic solutions of different mixtures. The heating methods used include heating by conventional methods, hot plates and a muffle furnace, a reflux-heating system and microwave-assisted digestion. The etching mixtures were prepared from a number of oxidizing acids and other dehydrating agents. The capability of each reagent to etch the layer completely and in a controlled manner was examined.

On etching the first layer, the OPyC, the reflux heating method gave the best results in removing the layer, its advantage being that the reaction can be carried out at temperatures of about 130 ºC for a long time without the loss of the acid. The experimental results demonstrated that a mixture composed of equal amounts of concentrated nitric and sulfuric acid mixed with chromium trioxide dissolves the OPyC layer completely. The most favourable experimental conditions for removal of OPyC

from a single coated fuel particle were identified and found to depend on the etching solution composition and etching temperature.

Light microscopy yielded first-hand information on the surface features of the samples. It allowed fast comparison of etched and untreated sample features. The outer surface of particles prior to chemical etching of the outer pyrolytic carbon layer appeared black in colour with an even surface compared to the etched surfaces which appeared to have an uneven metallic grey, shiny texture. The scanning electron microscope (SEM) examination of the chemically treated outer carbon layer samples gave information on the microstructure and it demonstrated that the outer pyrolytic carbon layer could be readily removed using a solution of $HNO_3/H_2SO_4/CrO_3$, leaving the exposed SiC layer. Complete removal of the layer was confirmed by energy dispersive X-ray spectroscopic (EDS) analysis of the particle surface.

For etching the second layer, the silicon carbide layer, microwave-assisted chemical etching was the only heating technique found to be useful. However, experimental results demonstrated that this method has limited ability to digest the sample completely. Also common chemical etchants were found to be ineffective for dissolving this layer. Only fluoride containing substances showed the potential to etch the layer. The results show that a mixture consisting of equal amounts of concentrated hydrofluoric and nitric acid under microwave heating at 200 ºC yielded partial removal of the coating and localized attack of the underlying coating layers.

The SEM analyses at different intervals of etching showed: partial removal of the layer, attack of the underlying layers and, in some instances, that attack started at grain boundaries and progressed to the intra-granular features. The SEM results provide evidence that etching of the silicon carbide layer is strongly influenced by its microstructure. From these findings, it is concluded that etching of the silicon carbide under the investigated experimental conditions yields undesirable results and that it does not provide complete removal of the layer. This method has the potential to etch the layer to some extent but has limitations.

Keywords: TRISO coated fuel particles; Silicon carbide; Pyrolytic carbon; Chemical etching; Microwave digestion

PUBLICATIONS EMANATING FROM THIS RESEARCH

The following conference contribution and article, which contain some of the results prescribed in this thesis, have been accepted as indicated:

1) Skolo, K.P. (2010). Stepwise disintegration of HTR simulated coated fuel particle. International Youth Nuclear Congress. Cape Town, South Africa.
2) K.P Skolo, P. Jacobs, J.H. Venter, W. Klopper, P.L. Crouse (2011). Wet-chemical dissolution of TRISO-coated simulated high-temperature reactor fuel particles. *Journal of Nuclear Materials* 420, 342-346.

TABLE OF CONTENTS

LIST OF FIGURES

LIST OF TABLES

LIST OF ABBREVIATIONS

BSE	Back Scattered Electrons
CO_2	Carbon dioxide
CrO_3	Chromium trioxide
CVD	Chemical Vapour Deposition
EDS	Energy Dispersive X-ray Spectroscopy
FP	Fission Product
H_2SO_4	Sulphuric acid
$HClO_4$	Perchloric acid
HF	Hydrofluoric acid
HNO_3	Nitric acid
HTR	High Temperature Reactor
IPyC	Inner pyrolytic carbon
OPyC	Outer Pyrolytic Carbon
PBMR	Pebble Bed Modular Reactor
PyC	Pyrolytic Carbon
SE	Secondary Electrons
SEM	Scanning Electron Microscope
SiC	Silicon carbide
TRISO	Tri-Structural Isotropic
UC_2	Uranium carbide
UO_2	Uranium dioxide
XRD	X-Ray Diffraction

CHAPTER 1

INTRODUCTION AND BACKGROUND

1.1 HIGH-TEMPERATURE REACTORS

High-Temperature Nuclear Reactors (HTRs) are graphite moderated and helium cooled. They represent a version of the original High-Temperature Gas-Cooled Reactors (HTGR) which successfully operated in Germany till the 1970s. For the last few years there has been internationally renewed interest in HTRs as potential technology for production of electricity and hydrogen. The revival of this technology is due to unique features of HTRs such as high fuel burn up, modular design, safety characteristics and the potential to provide electricity cost effectively without increasing the impact on the environment. A benefit of HTRs also includes the potential use of direct heat from the reactor outlet with helium temperatures in the range of 850 to 900 ºC (Kendall & Bullock, 2004), which can be applied for a variety of industrial processes, such as oil extraction.

HTRs can be classified into two fuel design types namely fuel in the form of hexagonal prismatic blocks and fuel in the form of spherical fuel spheres. Both designs make use of spherical tri-structural isotropic (TRISO) coated fuel particles, with a diameter of approximately 1 mm as basic fuel components. The spherical TRISO coated particles are mechanically strong and resistant to irradiation (Nabielek et al., 2009). Ideally they can be used to temperatures up to 1600 ºC while maintaining their mechanical integrity. They also provide complete retention of radioactive fission products under normal and accidental conditions.

The innermost unit of the coated particle is the fuel kernel, the material consists normally of uranium dioxide (UO_2), with the uranium enriched up to 9.6% Uranium-235. Other fuel kernels containing oxides or carbides and their mixtures with plutonium, or thorium, are also used (Verfondern et al., 2007). The kernels are individually enclosed with multiple coating layers, starting with a porous carbon buffer, then an inner pyrolytic

carbon (IPyC) layer, followed by a layer of ceramic silicon carbide (SiC) and finally an outer pyrolytic carbon layer (OPyC).

In a pebble bed type HTR design approximately 15 000 TRISO particles are dispersed evenly in a spherical graphite matrix forming a 50 mm diameter core with a 5 mm outer region of graphite without particles. This fuel configuration is portrayed in Figure 1.

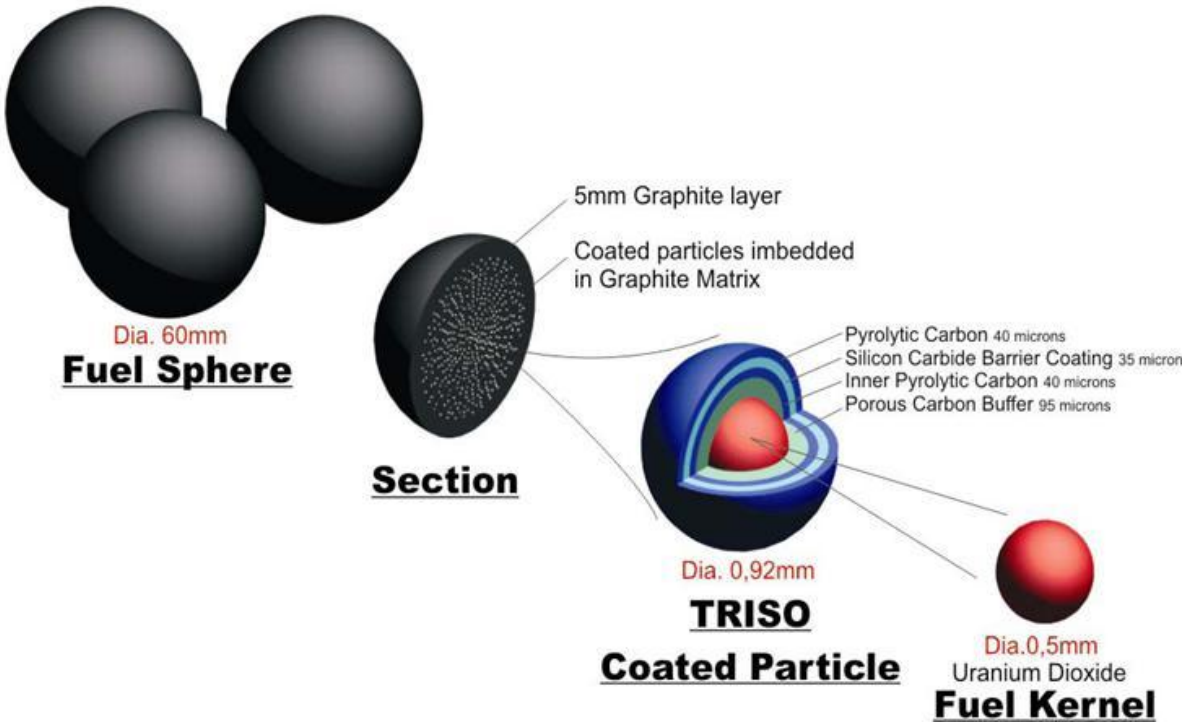

Figure 1: Schematic representation of PBMR fuel design

1.2 NUCLEAR FISSION PROCESS

During fission of uranium dioxide fuel, energy and a large number of fission products such as krypton, xenon, caesium, etc., are generated in the fuel kernel. The nuclear fission process is shown schematically in Figure 2. Oxygen atoms are also liberated in the kernel during the fission reaction (Markgraaff, 2009). Most of the fission products emit beta and gamma radiation, which makes the fuel highly radioactive. They are

considered a radiological hazard and therefore it is important to confine these products within the particle (Xu et al., 1995).

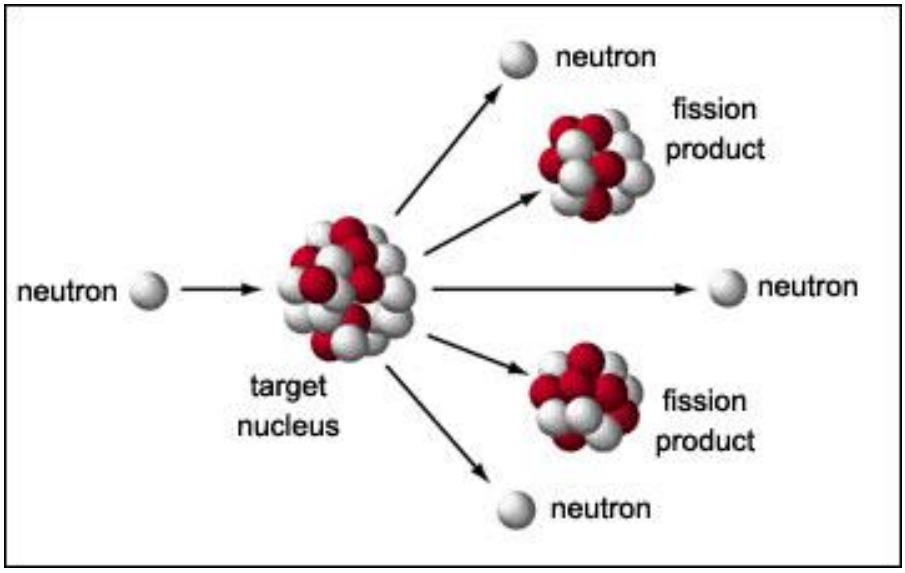

Figure 2: Schematic representation of a nuclear fission process

The kernel constitutes the first barrier to the release of the fission products. The released oxygen in the kernel binds with rare earth fission products (such as cerium, lanthanum, etc.) to form immobile oxides, thereby controlling their migration potential to the coating layers (IAEA, 1997). Products that fail to form stable oxides are released from the kernel through a diffusion process and are contained to a very high extent by the SiC layer (Nabielek et al., 1989).

The main function of the PyC and SiC coating layers is to ensure that fission products from the fission reaction are kept locked inside the particle preventing release of fission products generated during fission in the UO_2 fuel kernel (Minato et al., 2000). Among the coating layers, silicon carbide is the most essential of the barrier coatings (Kim et al., 2009). It acts as the main fission product barrier and provides structural strength and mechanical support for the coated particle.

Some of the fission products can escape through the PyC and SiC coating layers through diffusion or failed particle coatings (Inamati et al., 1985). Failed particles refer to (Inamati et al., 1985) particles with exposed kernels; or particles in which the silicon carbide coating has failed due to thermal decomposition or chemical attack by the fission products.

1.3 POSSIBLE FUEL FAILURE MECHANISMS

At high temperature and/or irradiation dose a coated particle is subjected to various forces, some of which are unfavourable to the chemical and mechanical stability of the coated particles (Markgraaff, 2009). Given that a coated particle is a retention barrier for the fission products, the chemical changes induced by irradiation could lead to particle failure and ultimately to the release of fission products. In the section below several performance-limiting mechanisms that lead to particle failure are described (Petti, 2006; Verfondern et al., 1990).

- **Impact of irradiation on pyrocarbon layers**: An irradiation effect on the pyrolytic carbon layers is reported to be chiefly responsible for the failure of the coated particles. Under irradiation both IPyC and OPyC layers shrink because of fast neutron exposure depending on neutron dose and irradiation temperature (Gulol et al., 2008; Rand, 2009). This shrinkage is observed in both radial and tangential directions. The shrinking behaviour of the OPyC causes it to push inward on the SiC layer while shrinkage of the IPyC results in pulling away from the SiC layer. The dimensional changes of the PyC layers will result in reduced tensile stress inside the SiC layer (Shenoy & Ellis, 2009; Miller et al., 2004). Figure 3 schematically shows the dimensional changes on a graphite crystal due to irradiation damage (Burchell & Snead, 2007).

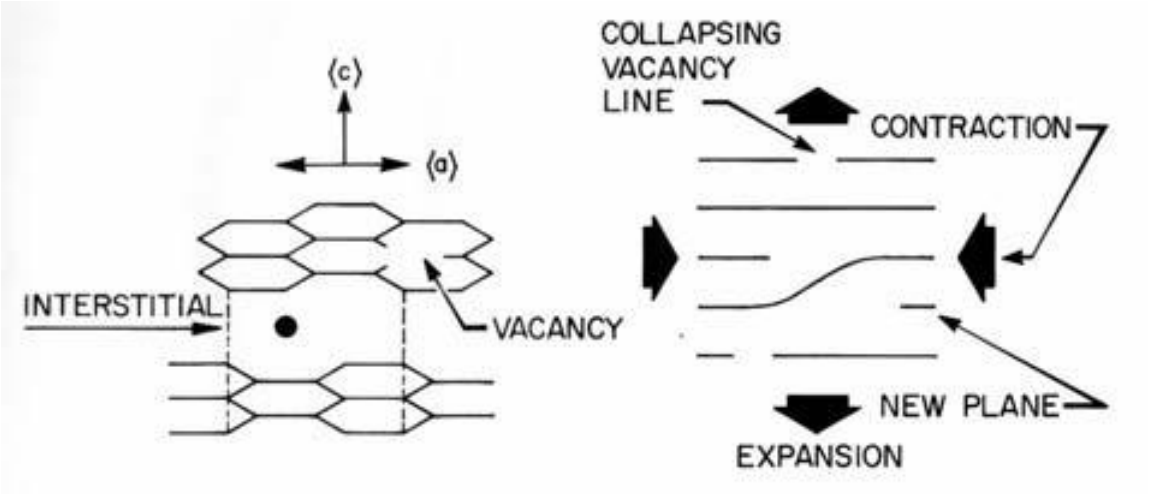

Figure 3: Crystal dimensional changes in graphite due to neutron irradiation (Burchell & Snead, 2007)

- **Fission product chemical interaction with SiC**: Chemical interactions of certain fission products liberated from the fuel kernel, such as palladium and some rare earth carbides, can potentially corrode and thin the silicon carbide coating (Verfondern et al., 1990).

- **Pressure-induced failure**: The fission gases and volatile products generated during irradiation are released from the kernel and build up inside the particle coatings. The built-up pressure inside the particle results in a tensile stress in the silicon carbide layer of the particle (Verfondern et al., 1990). This pressure vessel failure of a particle depends on multiple phenomena as illustrated in Figure 4 (Petti & Homan, 2006; Miller et al., 2004).

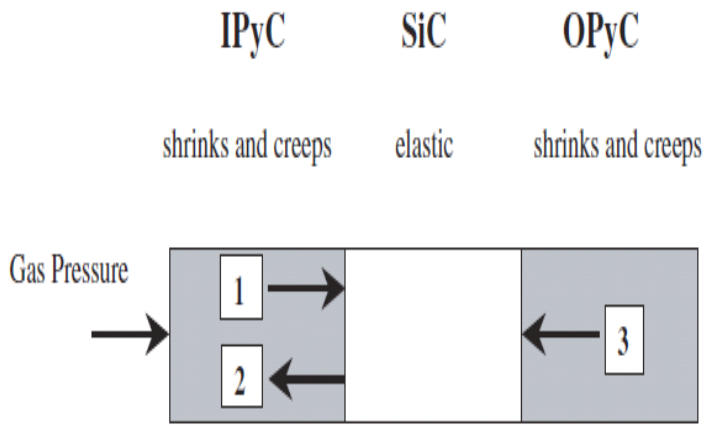

1. *Gas pressure is transmitted through the inner pyrolytic carbon layer*
2. *Inner pyrolytic carbon layer shrinks pulling away from the silicon carbide layer*
3. *Outer pyrolytic carbon layer shrinks pushing away on silicon carbide*

Figure 4: Behaviour of coating layers under irradiation (Miller et al., 2004)

Given that the SiC layer is the main load barrier (Ruggirello & Toscano, 2006), it is assumed (Verfondern et al., 1990; Petti & Homan, 2006) that if the stress in this layer is greater than its ultimate tensile strength, the event could result in simultaneous failure of all coating layers (IAEA, 1997). Figure 5 represents an image of a particle that failed due to overpressure.

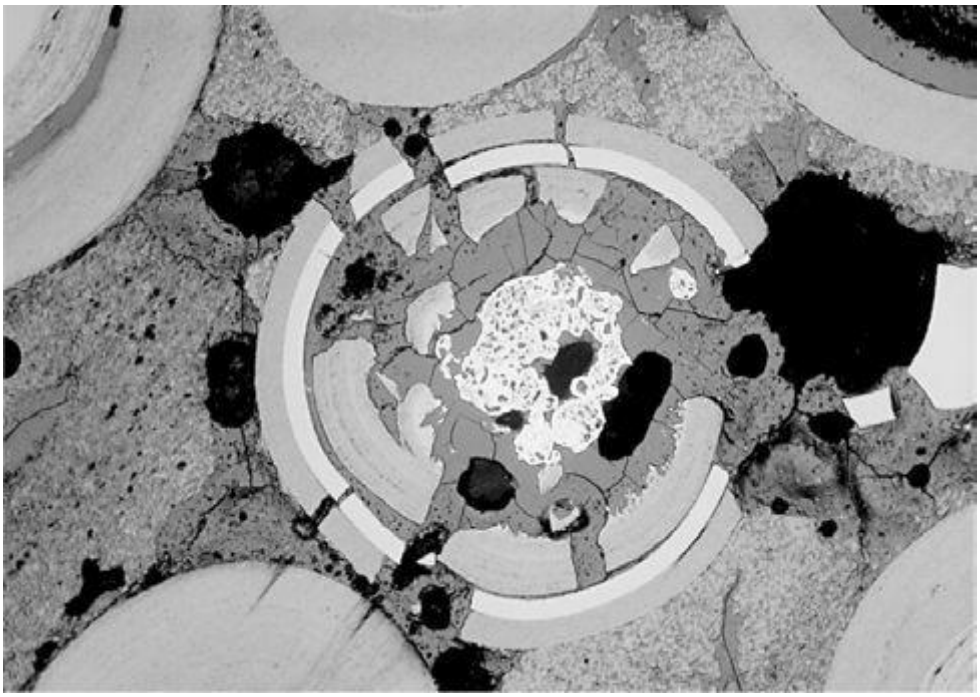

Figure 5: Microscopic view of section through a completely disintegrated TRISO coated particle (IAEA, 1997)

- **Kernel migration**: This effect, known as the “amoeba effect,” is postulated to occur when the fuel kernel relocates towards the direction of the coated particle layers (Verfondern et al., 1990). This movement occurs because of carbon monoxide transport within the particle in the presence of a temperature gradient. Since SiC is a brittle material, the movement of the kernel towards this layer could damage it completely, resulting in release of the fission products. This amoeba effect is more likely to occur in prismatic fuel elements than in pebble bed reactor fuel elements due to the presence of a higher temperature gradient (Gulol et al., 2008).

- **Diffusion through coatings**: Certain fission products within a fuel particle may escape either through diffusion or failed particle coatings.

These studies indicate that it is crucial to understand the behaviour of fission products in coating layers and their distribution as well as the failure of coating layers by interaction

with fission products. The particular interest in examining the behaviour of irradiated fuel is to check the manner in which fission products migrate and distribute in the coating layers (Fukuda & Iwamoto, 1975). The information obtained from the distribution can provide insight into the underlying physical and chemical mechanisms responsible for the coated particle failure.

One way to ascertain the distribution and migration of fission products in coating layers of the coated particles is by separating the layers in sequence. If a reliable technique is employed to obtain uniform removal of each layer, the concentration of fission products associated with each layer can be determined and analysed.

The removal of the coating layers has been studied by several researchers. Examples of techniques are the use of ion sputtering (Betz et al., 1971), chemical removal with chromium oxide dissolved in sulfuric acid and hydrofluoric acid at 140 °C (Chunhe et al., 2004), and thermal oxidation of carbon layers at 600 °C and 800 °C followed by crushing of the silicon carbide layer (Grambow et al., 2006; Fukuda & Iwamoto 1975; Delcul et al., 2002). The removal of the silicon carbide layer by molten salts has also been studied by Fukuda & Iwamoto (1975). The ion sputtering method does not provide sufficiently uniform removal of the material and moreover is not effective at low concentrations of fission products and fission materials (Betz et al., 1971).

The carbon layers can be readily removed by thermal oxidation (Grambow et al., 2006; Delcul et al., 2002). However, EDS studies by Grambow et al.(2006) showed that the removal of the carbon layers at 600 °C causes partial oxidation of the SiC layer. The focus in these studies was the determination of fission products in the removed contents of irradiated fuel particle coatings.

Layer-by-layer removal of the coatings of the particle is considered difficult regardless of the method employed. This is due to the chemical properties and strength of the coatings, in particular the silicon carbide layer, which is known to react poorly with acids and bases and is rigid (van Dorp et al., 2007). The size of the coated particle also has an impact on the method chosen. The particle has a nominal diameter of about 1 mm

with layer thickness ranging from 35 to 95 microns. This size makes separation by mechanical methods such as cracking difficult. Also for irradiated fuel, removal of the layers by cracking could require the use of expensive tools and extensive automation to avoid human contact.

1.4 AIM OF THE STUDY

The aim of this research was to investigate the possible use of wet chemical etching methods for removing the coatings of the coated particle layer by layer. The approach and objectives of the project was be based on the fundamentals of the chemical etching process, and its capability to remove the individual layers of the coated particles in sequence.

The objectives of this investigation were:

- To investigate step-by-step chemical etching of coated particle coatings
- To establish in detail optimum parameters for controlled dissolution of irradiated fuel

Experimental work was carried out on coated particles containing tetragonally stabilized zirconia kernels (also inaccurately known as zirconium kernels). The result of this study was used to evaluate whether the chemical etching technique is capable of removing the coating layers of irradiated particles for determination of fission products distribution and migration in irradiated fuel.

Characterization of the material microstructure and morphology during and after the etching process have been investigated by the following techniques: optical microscopy, scanning electron microscopy equipped with an energy-dispersive X-ray system and X-ray diffraction.

CHAPTER 2

PBMR FUEL

2.1 PBMR FUEL STRUCTURE

The spherical fuel elements for modular pebble bed reactors are manufactured from A3-3 graphite matrix material. The graphite matrix consists of natural graphite powder, electro-graphite powder and a phenolic resin. In this matrix, about 15 000 of the TRISO coated fuel particles are dispersed evenly forming a 50 mm diameter inner core with a 5 mm thick outer particle-free graphite layer. The 5 mm outer fuel-free region protects the inner core from damage against external forces during fuel fabrication. The matrix material functions as a moderator for fission neutrons, provides good thermal properties and stabilizes the coated particles in the sphere. The fuel-free matrix also protects the coated particles against damage from outside mechanical effects during loading of the fuel (Nabielek et al., 2009).

A TRISO particle consists of a fissionable uranium dioxide (UO_2) fuel kernel, typically in the order of 500 μm and is encased in various layers. These layers consist of a porous carbon buffer layer and two dense layers of pyrolytic carbon. Sandwiched between the dense pyrocarbon layers is silicon carbide, a ceramic layer.

2.2 TRISO COATED FUEL PARTICLES

2.2.1 Overview of HTR Coated Fuel Particles

TRISO coated fuel particles are fundamental fuel unit components for high temperature reactors. They are designed to ensure mechanical stability and retain metallic and gaseous fission products under normal and accident conditions.

The coating layers that make up the TRISO coated particle are manufactured by a chemical vapour deposition process carried out in fluidized bed coaters. Deposited on

top of the fuel kernel sequentially, the layers are a porous pyrolytic carbon buffer, inner pyrolytic carbon (IPyC), a silicon carbide (SiC) layer and an outer pyrolytic carbon layer (OPyC). A scanning electron micrograph (SEM) of a cracked open coated particle with the entire layer system is shown in Figure 6.

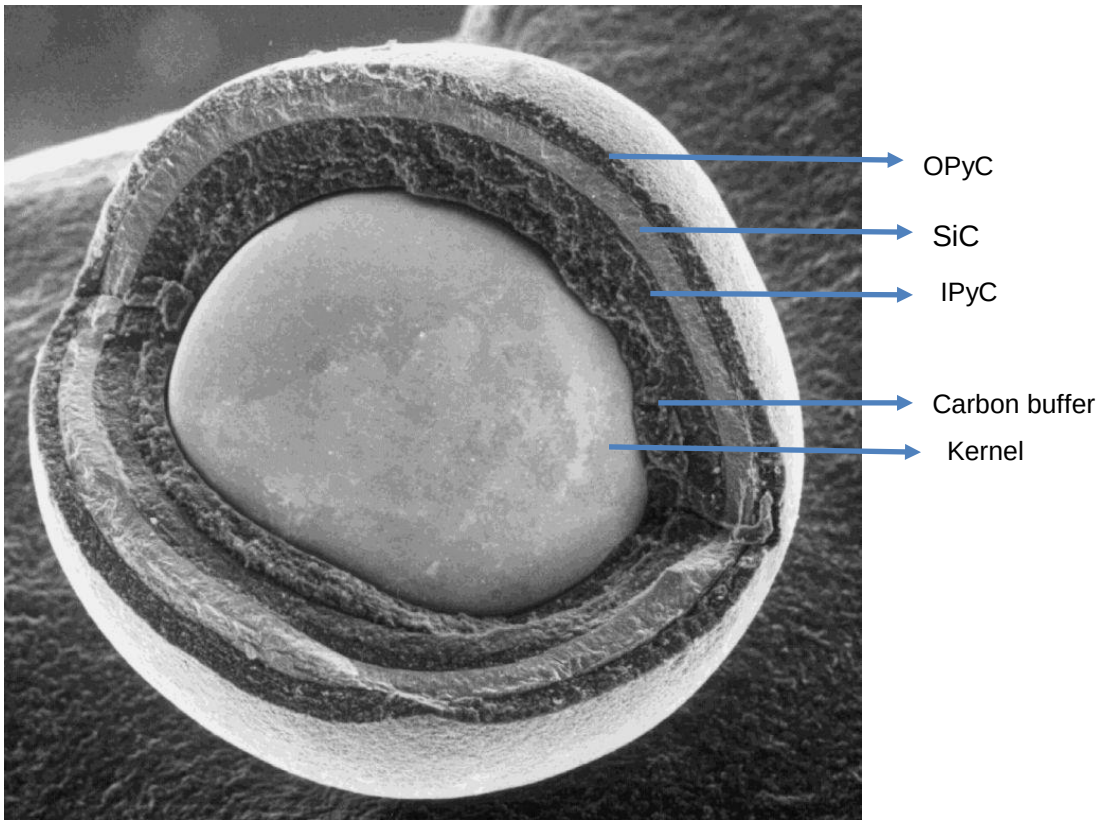

Figure 6: SEM micrograph of a TRISO coated particle (Languille, 2002)

The total system of coating layers is termed a tri-structural isotropic (TRISO) coating. The term refers to a coating system that makes use of three types of layers namely; low density pyrolytic carbon, high density and pyrolytic carbon for the inner and outer layers and silicon carbide (Shenoy and Ellis, 2009).

2.2.2 Fabrication of Coating Layers

The TRISO coating results from decomposition of different gas phase molecules in a heated furnace, a process commonly known as chemical vapour deposition (CVD). The CVD process for deposition of the four coating layers is as follows: The porous buffer layer is deposited from acetylene gas (C_2H_2) and argon at around 1250 ^oC. A mixture of acetylene and propylene ($C_2H_2 + C_3H_6$) in the presence of argon gas is used for the deposition of the IPyC and OPyC layers at around 1300 ^oC and the SiC layer is deposited by decomposition of methyltrichlorosilane in the presence of hydrogen ($CH_3SiCl_3 + H_2$) at around 1500 ^oC (Barry, 2008). The chemical deposition sequence during fabrication of the TRISO coated particles is shown in Figure 7.

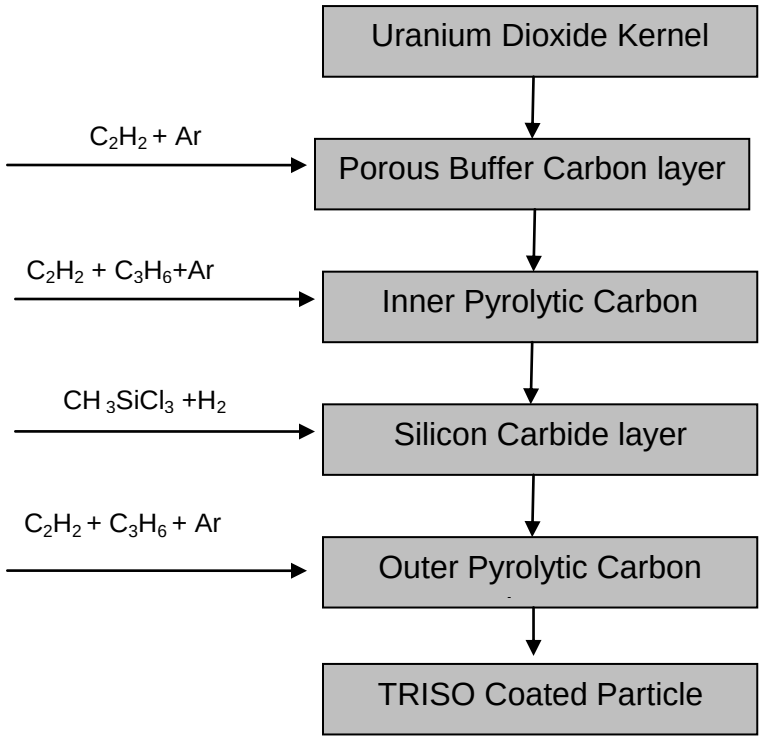

Figure 7: Input gases during fabrication of TRISO coated particles (Ablitzer et al., 2007)

2.2.3 Basic Functions of Coated Particle Components

Pyrolytic carbon layers provide retention of noble gas fission products while silicon carbide is regarded as the most important layer of the coating system since it acts as the major barrier to metallic fission products and gaseous fission products (Verfondern et al., 2007).

The fuel kernel contains the fissile material and it produces energy from the fission process. During neutron irradiation, the kernel produces internal pressure in the coated particles and migration of some generated fission products into the coating layers.

The pyrolytic carbon buffer is a low-density porous material, around 95 µm thick. The purpose of this layer is to provide voids to accommodate released fission gases and to distort to accommodate swelling of the fuel kernel during irradiation.

The IPyC layer is a dense form of pyrolytic carbon deposited on the surface of the buffer layer, 40 to 45 µm in thickness. The IPyC layer protects the fuel kernel from reacting with chlorine, in the form of hydrogen chloride, produced during deposition of the SiC layer (Snead et al., 2007). It also provides a good surface for depositioning of the SiC layer and provides retention of noble gases. This layer also plays a role in the mechanical stress distribution within the coated particle.

Deposited on the surface of the IPyC is a high strength, cubic crystalline form of silicon carbide, approximately 35 to 40 µm thick. This layer is considered the most critical layer in the performance of the fuel particle, as it serves as the main barrier to retain fission products. The SiC layer also is the main load-bearing component of the coating layers (Ruggirello & Toscano, 2006). The SiC layer also provides structural support required to withstand the internal gas pressure in the particle developed during irradiation (Nabielek et al., 2009). The OPyC layer acts as the final barrier to the release of gaseous fission products. It consists of the same material as the IPyC with a thickness of 40 to 45 µm. This layer is directly deposited on top of the brittle SiC material and thus protects it during fuel fabrication and fuel handling prior to fuel element fabrication.

CHAPTER 3

AN OVERVIEW OF THE PROPERTIES OF THE COATING LAYERS OF THE TRISO COATED PARTICLE

The carbon and silicon carbide used in TRISO coating systems are employed due to their excellent characteristics. These include: good irradiation stability, high thermal stability, good mechanical stability up to high temperatures, and resistance to chemical attack. The good chemical resistance in these materials, however, may cause potential problems when spherical layers have to be removed by means of chemicals. In order to make informed decisions in this regard, a good knowledge of their chemical properties is essential.

3.1 CARBON AND ITS ALLOTROPIC FORMS

Carbon is the lightest chemical element in group 6 with a ground state configuration of $1s^2 2s^2 2p^2$. Therefore, carbon has four electrons in the outer shell to form several types of covalent chemical bonds. Carbon is very different from most other elements because it has the ability to form stable bonds with itself in different ways, leading to large series of compounds. Its electron configuration allows the formation of several allotropic forms.

The two well-defined allotropic forms of carbon are diamond and graphite, other forms include fullerenes, nanotubes and synthetic forms of carbon. Carbon allotropes differ in the way in which the atoms are bonded and this has a profound effect on their chemical and physical properties (Pierson, 1999). For example, diamond is highly transparent and extremely hard, due to single carbon-carbon bonds in its crystal structure. Graphite on the other hand is a soft material with lubricating properties. The carbon atoms in graphite are held by weak forces; as a result the layers slide over one another easily, thus creating a lubricant effect.

3.2 CARBON GRAPHITE MATERIALS IMPORTANT TO NUCLEAR REACTORS

Carbon graphite materials vital to nuclear reactors, particularly high temperature reactors, include nuclear graphite and pyrolytic carbon.

3.2.1 NUCLEAR GRAPHITE

The graphite material used in nuclear reactors is referred to as nuclear graphite ((Carter and Eggleston, 1955; Baker, 1971 and Sharma, 1995). Graphite is used because of its good moderating properties; it slows down fast moving neutrons to sustain the nuclear fission reaction (Marsden et al., 2005). It is amongst a list of potentially good moderators such as beryllium, water and deuterium (Burchell, 2001). Ideally a moderator should have the following characteristics: (i) preferably it must be inexpensive; (ii) it must not react with neutrons and only absorb them to a small extent; (iii) the fast neutrons should be slowed very quickly with a few collisions in the moderator; and (iv) have a low atomic weight. In graphite, most of these requirements are fulfilled. Graphite also act as a structural component, providing thermal and neutron reflection as well as shielding.

3.2.1.1 Atomic Structure of Graphite

Graphite is a layered compound as shown schematically in Figure 8. The carbon atoms in a layer are arranged hexagonally, sp^2 hybridized and are strongly covalently bonded to 3 other carbon atoms. The bond between carbon layers is weak van der Waals bonding, which permits easy sliding of the planes over another (Chung, 1994). The interlayer spacing between basal planes is 0.335 nm, more than twice the spacing between atoms 0.142 nm (Pierson, 1993).

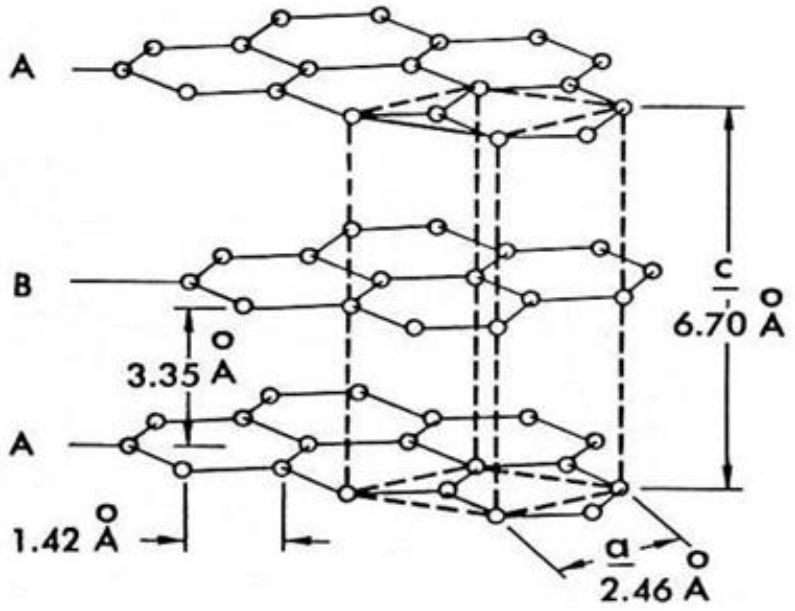

Figure 8: Schematic crystal structure of graphite (Rand, 2009)

3.2.1.2 Physical and Mechanical Properties of Graphite

It is vital to mention that the graphite material (nuclear graphite) used in nuclear reactors has different properties compared to those of natural graphite. The difference in properties is brought about by the bonding condition of the carbon atoms within the lattice as well as the manufacturing process used. Nuclear graphite is manufactured from petroleum or natural pitch cokes. The stages of the nuclear graphite manufacturing process are highlighted in Figure 9.

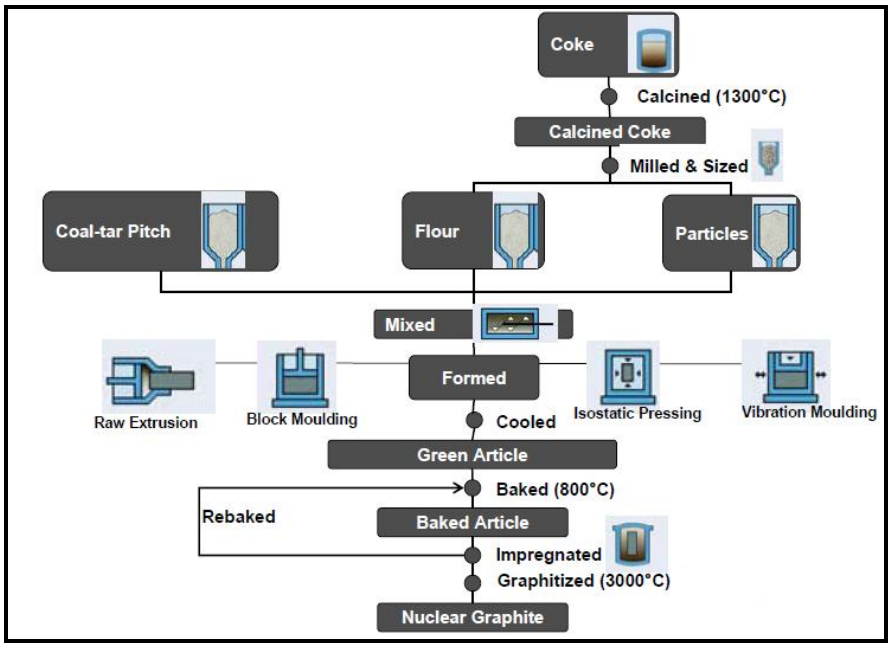

Figure 9: Manufacturing process of nuclear graphite (Jones & Marsden, 2010)

The nuclear graphite material manufactured by the process shown in Figure 9 has the following properties (Pierson, 1999; Jones & Marsden, 2010; Marsden et al., 2005, Rand, 2009; Wickham & Haag, 2004):

- A poly-granular and poly-crystalline microstructure.
- In oxidising atmosphere the material starts to be oxidised at 500 to 600 ^{0}C. Non-graphitised carbon graphite materials are only stable up to 350 ^{o}C.
- The density will be in the range of 1.6 - 1.8 g/cm^{3}, the density is less compared to the theoretical density of 2.265 g/cm^{3} for natural graphite. The manufactured graphite material is more porous compared to the natural graphite.
- The material has high mechanical strength and stability at high temperatures (Strength need to be in the range of 20 MPa)

The strength is maintained at temperatures approaching 2000 ^{o}C. Generally, when materials are heated, they tend to soften and the strength falls with an increase in temperature, but with nuclear graphite it is the opposite. The strength increases with an increase in temperature, until a maximum is reached at about 2500 ^{o}C, after which the

strength decreases (Rand, 2009). An example of such behaviour is shown in Figure 10, for various graphites heated to about 3200 ºC.

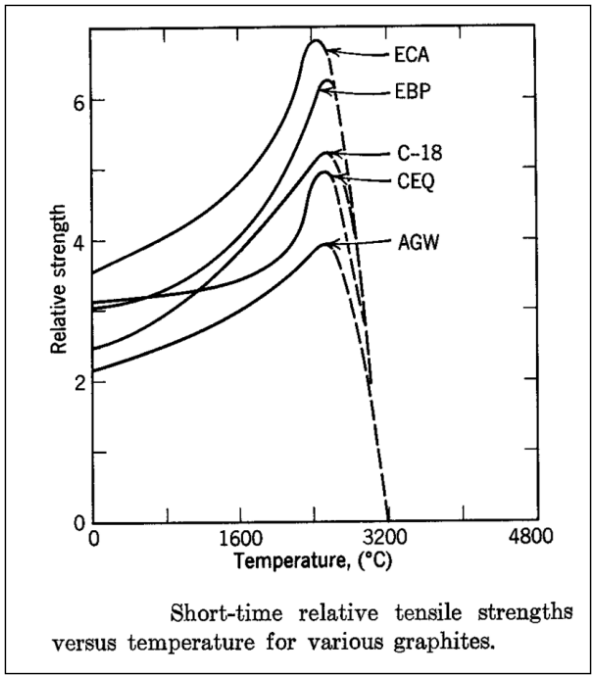

Figure 10: Tensile strength for various types of graphite vs. temperature (Rand, 2009)

3.2.2 PYROLYTIC CARBON

3.2.2.1 Synthesis of Pyrolytic Carbon

Pyrolytic carbon (PyC) is also a synthetic form of carbon graphite material. In nuclear reactors it is used as a coating layer material of high temperature reactor fuel particles to support retention of fission products inside the fuel particle.

Pyrolytic carbon in fuel particles is produced by a chemical vapour deposition (CVD) process, as mentioned, where a mixture of hydrocarbons such as acetylene and propylene is decomposed at temperatures above 1000 ºC. A commonly used CVD reaction for production of PyC layers includes decomposition of acetylene for producing the porous carbon buffer layer and a mixture of acetylene and propylene in the presence of argon gas for the dense pyrocarbon layers.

The structure and properties of the carbon products formed from the CVD process can vary significantly as function of the deposition conditions (Lopez-Honorato et al, 2009). The influential parameters identified by Bokros (1969) are variations in deposition temperature, hydrocarbon type used and concentration of the hydrocarbon. Of these the deposition temperature is the most important parameter.

3.2.1.3 The Structure of Pyrolytic Carbon

Pyrolytic carbon (PyC) has a poorly defined crystalline structure with disordered carbon atoms (Dauskardt, 1993); hence this carbon material is classified as turbostratic carbon. Its structure is related to that of graphite (Figure 8). Similar to graphite the carbon atoms are hexagonally arranged, i.e. they are predominantly sp^2 hybridized, but in pyrolytic carbon the layers are not perfectly arranged (Figure 11).

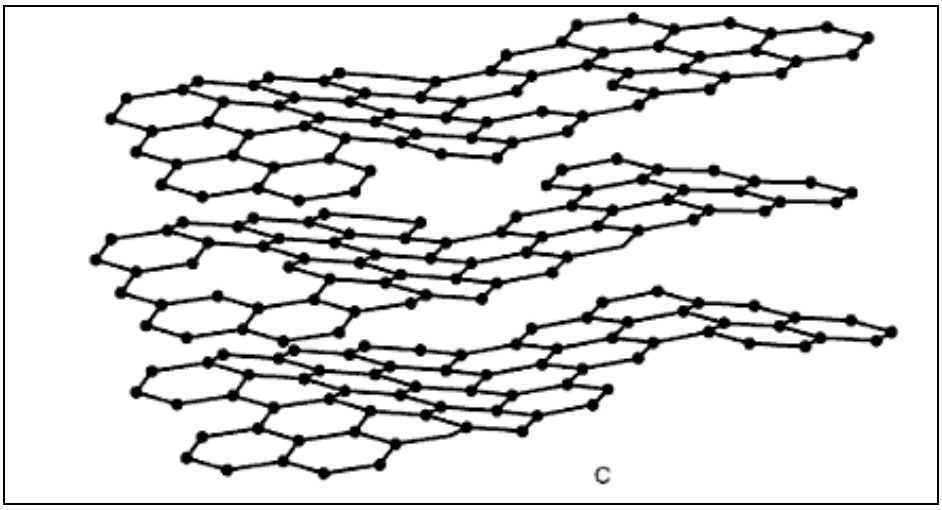

Figure 11: Turbostratic carbon, layers arranged without order (More et al., 2004)

3.2.1.4 Properties of Pyrolytic Carbon

PyC has excellent properties such as good mechanical strength, high corrosion resistance, good chemical inertness and stable to irradiation, and high density (>2 g/cm^3, depending on the production technique used). Pyrolytic carbon is mechanically harder than graphite. In graphite, the planes can easily slide over one

another while in pyrolytic carbon the ability of planes to slip is inhibited due to distortion. In the study by Bhat (2002), the mechanical strength of pyrolytic carbon, Table 1, is shown to be higher compared to other forms of carbon; glassy carbon and graphite.

Table 1: Mechanical properties of carbon materials (Bhat, 2002)

Property	Graphite	Glassy Carbon	Pyrolytic Carbon
Density (g/cm^3)	1.5 - 1.9	1.5	1.5 - 2.0
Elastic Modulus (GPA)	24	24	28
Compressive Strength (MPA)	138	172	517

Figure 12 displays a variation of strengths for carbon/graphite materials. The polynuclear graphites are shown to have relatively low modulus and strength (Rand, 2009). This is due to the porosity nature of the poly-granular graphites.

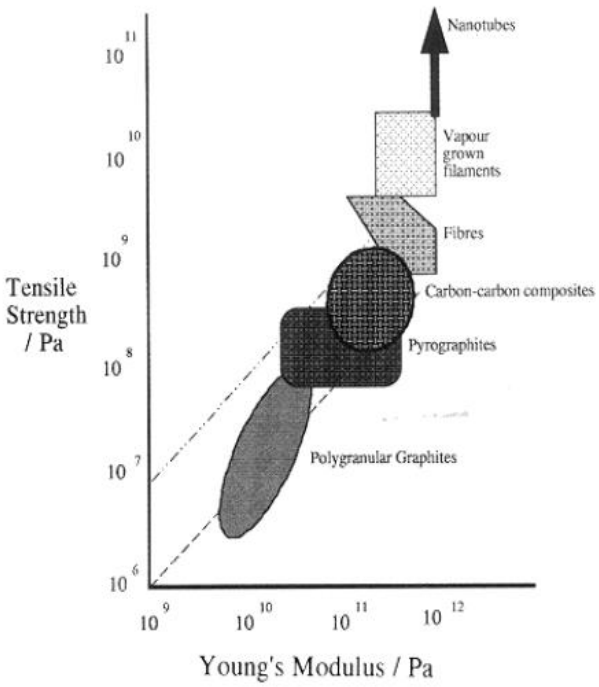

Figure 12: Range of moduli and strengths of carbon/graphite materials (Rand, 2009)

3.2.2 CHEMICAL PROPERTIES OF GRAPHITE AND PYROLYTIC CARBON

Chemically, carbon-based materials are of low reactivity, they are sufficiently resistant to most chemical environments especially at low temperatures. They are insoluble in dilute acids and bases, and do not react with corrosive gases (Pierson, 1993). Their chemical activity increases in the presence of strong oxidising agents such as sulfuric acid, nitric acid and perchloric acid, and in an oxygen environment at temperatures above 500 °C they can be oxidized (Buzelli & Mosen, 1977).

A mixture of nitric acid mixed with potassium dichromate (Fukuda & Iwamoto, 1977) can dissolve pyrolytic carbon material obtained by the CVD process. Hunter et al. (1990) used a chemically heated mixture of fuming nitric acid and fuming sulfuric acid to dissolve PyC layers.

Strong oxidising acids such as nitric acid, perchloric acid, and sulfuric acid (Buzelli & Mosen, 1977; Pierson, 1993) easily attack graphite. The reaction with hot sulfuric acid proceeds as follows (Pierson, 1993):

$$C_{(s)} + 2H_2SO_{4\,(l)} \rightarrow CO_{2\,(g)} + 2H_2O_{(g)} + 2SO_{2\,(g)} \qquad (3.1)$$

In nitric acid media graphite also decomposes to form carbon dioxide (Pierson, 1993):

$$C_{(s)} + 4HNO_{3\,(aq)} \rightarrow CO_{2\,(g)} + 4NO_{2\,(g)} + 2H_2O_{(l)} \qquad (3.2)$$

In the case of perchloric acid, chlorine is the oxidant. From its high oxidation state (+7) in the perchlorate ion, it can be reduced to several lower states, acting as oxidant, i.e. an electron acceptor (Cotton and Wilkinson, 1980).

A study by Choi & Leu (1998), showed that the nitric acid molecules are able to penetrate between the 0.335 nm layers in graphite and the reaction takes place both on the outer surface plane and between the graphite layers.

Other atoms such as potassium, lithium, oxygen, bromine, etc., are also known to penetrate between graphite planes in a layered pattern. The compounds formed by this

reaction are called graphite intercalation compounds (Boehm et al. 1994; Yan et al., 2004). Figure 13 illustrates how lithium ions are intercalated in a graphene layer.

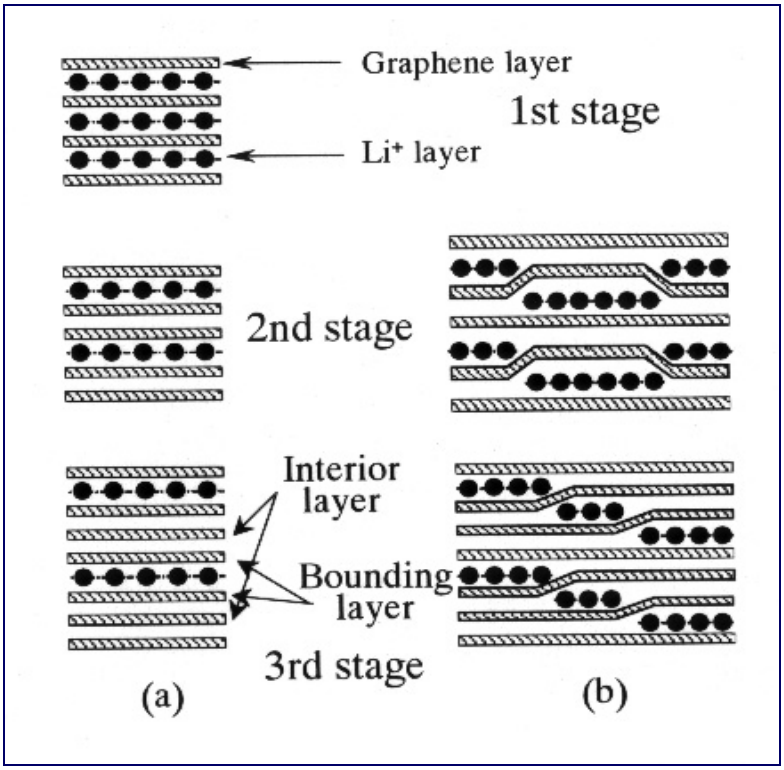

Figure 13: Lithium ions intercalating between graphene layer (Rand, 2009)

The literature shows that carbon materials such as graphite and pyrolytic carbon have different crystalline structures resulting in different chemical and physical properties. The fact that only very strong oxidising agents (nitric acid, sulphuric, and perchloric acid) were used in published methods dealing with dissolution (Fukuda & Iwamoto, 1977; Buzelli & Mosen, 1977; Pierson, 1993) point to the chemical stability of the PyC.

3.3 INTRODUCTION TO SILICON CARBIDE

Silicon carbide (SiC) is a ceramic compound, widely known as a capable semiconductor material with good electrical and mechanical properties. Also it has excellent potential for use in harsh environmental conditions such as high temperature and high level of radiation (Brink et al., 2009). Furthermore, this material is extremely important in structural applications. For example in TRISO coating it is utilized to provide structural strength and dimensional stability to the HTR coated particles.

3.4 Silicon Carbide Production

SiC rarely occurs naturally. In 1891 it was first produced by the Acheson process in which a mixture of silica sand and carbon (coke form) was electrically heated and reacted in an electric furnace at 2700 ºC (Somiya & Inomata, 1988). The Acheson reaction proceeds as follows (Snead et al., 2007):

$$SiO_{2\,(s)} + 3C_{(s)} \rightarrow SiC_{(s)} + 2CO_{(g)} \qquad (3.3)$$

Silicon carbide can also be produced through direct sintering, gas phase reaction, chemical vapour deposition and other techniques. Among these techniques chemical vapour deposition (CVD) is the preferred coating method for preparing the SiC coating of the HTR particles (Helary et al., 2008; Kim et al., 2007; Sone et al., 2000). The advantage of using this process is that it results in cubic crystalline SiC (β -SiC) with high purity, a material known to be compatible with nuclear reactors and highly suitable for use in high temperatures. However, the characteristics of the silicon carbide coating or material obtained by the CVD process depend strongly on deposition conditions such as gas flow rate, concentration of coating gas, as well as coating temperature (Kim et al., 2009). CVD-SiC for use in coated particles is usually deposited by the decomposition of methyltrichlorosilane (CH_3SiCl_3) combined with hydrogen as carrier gas at a temperature range of 1500 ºC to 1650 ºC (Ablitzer et al., 2007; Lopez Honorato et al., 2009). The reaction proceeds as follows:

$$CH_3SiCl_{3\,(g)} + H_{2\,(g)} \rightarrow SiC_{(s)} + 3HCl_{(g)} + H_{2\,(g)} \qquad (3.4)$$

Other coating techniques result in crystalline silicon carbide with low purity. For example the Acheson process produces a material that contains impurities such as aluminium and iron.

3.5 Structure and Properties Of Silicon Carbide

3.6 Silicon Carbide Crystal Structure

The crystal structure of silicon carbide consists of a covalently bonded tetrahedral structure, where each silicon atom is tetrahedrally bonded to four carbon atoms or vice-versa, Figure 14 (Saddow & Argawal, 2004). The bonding distance between carbon-carbon atoms is large (0.308 nm) compared to a chemical bond between a carbon atom and a silicon atom (0.189 nm).

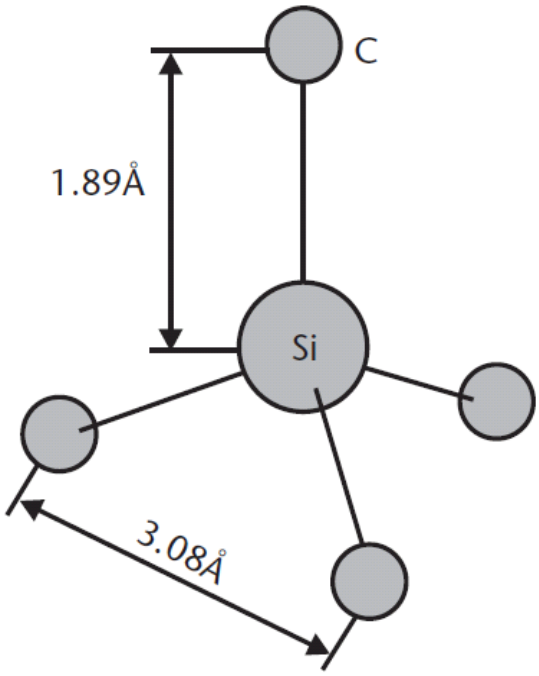

Figure 14: Schematic structure of SiC crystal (Saddow & Argawal, 2004)

Silicon carbide is known to exist in numerous polytypes, with the same chemical composition but differing from one another in the stacking arrangements of the silicon and carbon atoms (Kimoto & Matsunami, 2004). Only few polytypes are considered to be of technological importance (Saddow & Argawal, 2004) namely the 3C, 4H, 6H, and 15R-SiC. In these notations (Zappe, 2006), the number stands for the number of silicon and carbon double layers that it takes to build a unit cell of the crystal while the letters denotes the crystal structure. The letters C, H, and R represent cubic, hexagonal, and rhombohedral crystals respectively. The hexagonal and rhombohedral forms are collectively referred to as alpha (α) polytypes denoted by α-SiC; the cubic polytype are denoted as beta (β). These crystal structures are schematically illustrated in Figure 15. The cubic polytype is the type of material commonly used for silicon carbide coating of the HTR coated particles.

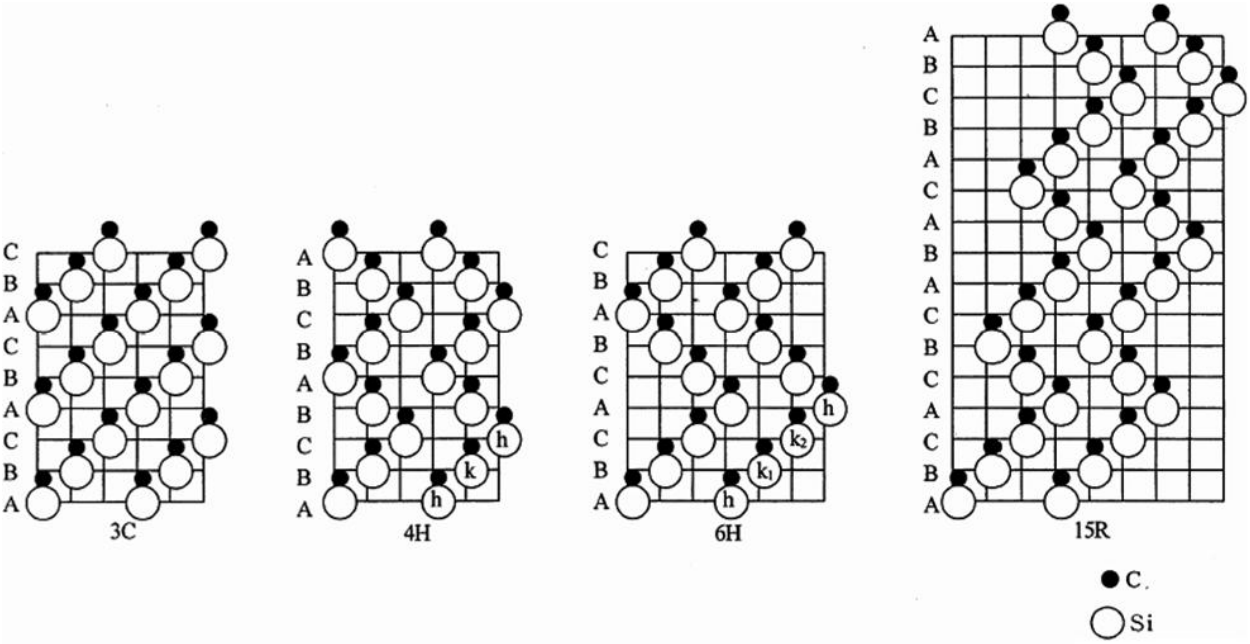

Figure 15: Crystal structure of SiC polytypes: 3C, 4H, 6H and 15R-SiC (Snead et al., 2007)

3.7 Properties of Silicon Carbide

Silicon carbide has outstanding properties such as excellent mechanical strength (mho hardness >9), resistance to oxidation, corrosion and chemical attack, high temperature stability (unstable only above ~2 000 ºC) as well good irradiation stability (Kim et al., 2007).

Silicon carbide consists of low atomic number elements and hence has low density (3.21 g cm^{-3}) and is a good thermal conductor. In comparison to other ceramics, silicon carbide has a wide band-gap that ranges from 2.3 eV to 3.3 eV. This property makes it a suitable material for high temperature, high power and high frequency applications (Saddow & Argawal, 2004).

Silicon carbide is chemically extremely resistant. It is not easily attacked when reacting with chemicals such as hydrochloric and sulfuric acid, including a boiling acid aqua regia at normal pressures (van Dorp et al., 2007; Pearton, 2006; Zinovev et al., 2006). Silicon carbide can be chemically etched with a mixture of HF/Na_2O_2 at 80 °C (Gabouze et al., 2009). In the presence of oxygen at 850 °C, it is oxidized to SiO_2 (Yamada & Mohri, 1998). Its chemical reactivity is strongly dependent on factors such as microstructure, the presence of impurities and the fabrication route used to produce the SiC material (Batchelor et al., 2002).

CHAPTER 4

REMOVAL METHODS FOR COATED PARTICLE LAYERS

4.1 INTRODUCTION

The function of particle coatings as stated in Chapter 2 is to contain the fission products (FPs) generated in the fuel kernel. The migration behaviour of these products requires analysis of their distributions in the particle coatings. Several methods exist for the removal of layers to obtain the distribution of the FPs. Previously reported removal methods include: mechanical separation, ion sputtering (Betz et al., 1971), chemical etching (Fukuda & Iwamoto, 1977), molten salt etching, removal by laser evaporation and oxidation of carbon layers followed by crushing the silicon carbide layer.

After irradiation, the particles embedded in the graphite matrix must be separated from the graphite fuel spheres. This can be achieved by destruction of the graphite, without harming the particles. Selective destruction of graphite may be obtained using: (i) chemical reactions of bromine, bromide-iodine, caesium, iodine-chlorine, alkaline metals and metal halides, etc.; (ii) methods based on the differential attack rates by a mixture of oxidising substances with strong acid; and (iii) electrochemical methods. A detailed description of these methods is given by (Reitsamer et al., sa).

Several techniques to remove layers from coated particles have been investigated for their capability to determine distribution of FPs.

4.2 PREVIOUSLY INVESTIGATED REMOVAL METHODS

4.2.1 Chemical Methods

In the study by Hunter et al. (1990), methods used to remove layers involved a combination of cracking and chemical dissolution. The particles retrieved from graphite fuel elements were cracked mechanically to separate the coatings from the fuel kernels. The kernel was then dissolved in hot concentrated nitric acid and the resulting solution

was analyzed for the presence of fission products. A mixture of fuming nitric and sulfuric acid, 1 ml each, was used simultaneously to dissolve and separate the fragmented PyC layers (porous PyC, IPyC and OPyC) from the silicon carbide layer.

According to their study, the PyC layers disintegrated in the acid, forming a black solution. After dissolution of the PyC layers, the remaining SiC layer fragments were washed and then analyzed by direct gamma spectrometry. No data on the removal rates or other experimental variables were given.

The removal method applied in the study is not complicated. The drawbacks of the method include simultaneous dissolution of the various PyC layers and the fact that FPs from the SiC layer can be released into the solution. This type of removal does not provide precise information on FP distribution associated with each layer.

The pyrolytic carbon layers of a single coated particle can also be dissolved in a potassium dichromate-nitric acid ($K_2Cr_2O_7$-HNO_3) solution at 140 ºC (Iwamoto & Fukuda, 1977). When this solution is used the removal of the layers is shown to be a time dependent function of layer thickness. Figure 16 shows the dissolution process of the particle layers in $K_2Cr_2O_7$-HNO_3 solution for the PyC layers, and the SiC layer in KOH-Na_2CO_3 solution.

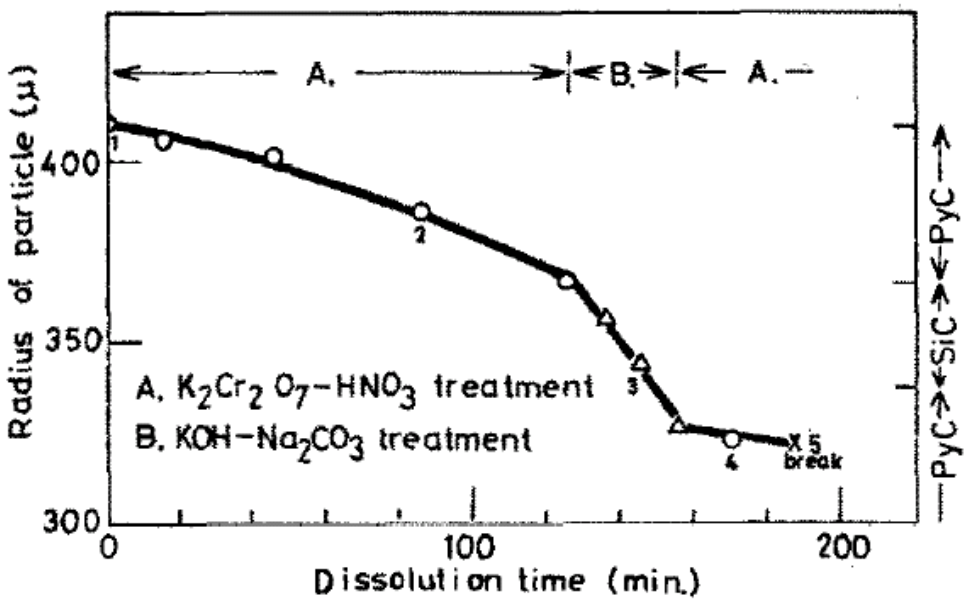

Figure 16: Dissolution process of coated particles in $K_2Cr_2O_7$-HNO_3 solution (Iwamoto & Fukuda, 1977)

The removal of silicon carbide layer was also studied using molten mixtures of potassium hydroxide (KOH) and sodium carbonate (Na_2CO_3) in the ratio 4:1 at 800 ºC (Fukuda & Iwamoto, 1976).

4.2.2 Removal by Sputtering

In the study by Betz et al. (1978), the ion sputtering process was used to remove the surface material of a coated particle to determine the distribution of fission products.

Sputtering is a process whereby ions from, for an example a focused ion beam, hit the surface of the material and knock atoms from their lattice positions. These sputtered atoms may leave the target surface as either atoms or ions. A schematic of the sputtering process is shown in Figure 17.

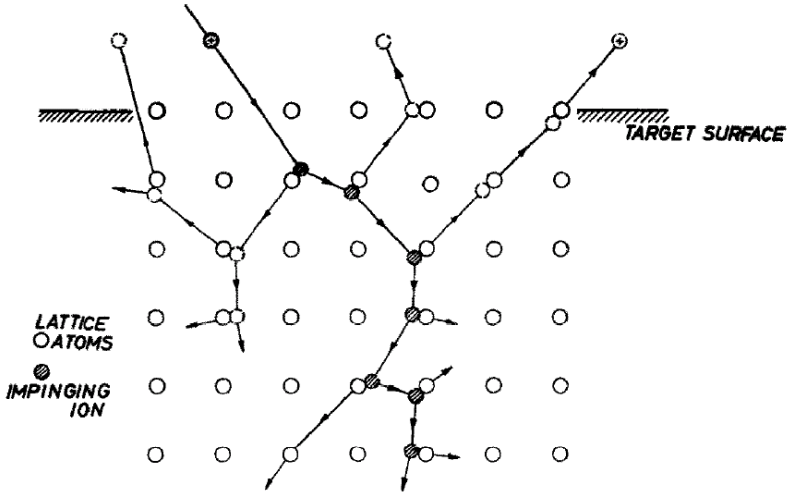

Figure 17: Schematic principle of the sputtering process (Betz et al., 1978)

The sputtering process makes use of the fact that fission products will be sputtered simultaneously with the lattice atoms of the coating layers. Sputtered material and species are then condensed onto a collecting material or container followed by analysis of FPs using detectors. The main limitation of this technique is the complexity and expense of the equipment required.

4.2.3 Removal by High Temperature Oxidation

The oxidation of carbon in air or oxygen at temperatures of 800 to 1100 ºC is the method that has been used extensively to destroy or deconsolidate carbon. This separation of irradiated carbon from particle coatings produces carbon dioxide as a by-product that needs to be treated by expensive and complicated off gas treatment systems (Delcul et al., 2002).

The removal of outer carbon layer from the particle has, for example, been performed by heat treatment in a thermo-gravimetric analysis (TGA) apparatus (Grambow et al., 2006). Oxidation of the layer under this treatment was completed by four cycles of heating to 600 ºC over 24 hours. Complete removal of the outer carbon layer was

confirmed by scanning electron microscope investigations. However, energy dispersive X-ray analysis of the sample showed that the SiC layer was partially affected by the oxidation as it indicated the presence of silicon dioxide (Grambow et al., 2006).

The experiments on removal of carbon by high temperature oxidation were researched for reprocessing of irradiated fuel. It is not clear if the distribution of FPs can be determined by this method.

4.2.4 Other Etching Techniques for SiC

Information regarding etching or dissolution of SiC is mainly available for surface treatment of semiconductor devices to reveal and investigate defects such as dislocations, stacking faults and surface abnormalities (Harris, 1995). Semiconductor material usually consists of thin layers of single crystals or polycrystalline material (Landolt et al., 1984). The study by Landolt et al., (1984) indicated that SiC generally reacts poorly with acid and alkaline solutions at room temperatures and also that its chemical behaviour strongly depends on type of the semiconductor material used.

Cubic SiC whiskers produced by carbothermal synthesis were etched electrolytically in a solution of 47-52 % hydrofluoric acid and 70 % nitric acid at 100 ºC for 3 hours (Cambaz et al., 2005). The experimental results of this study revealed that the β-sic crystal is preferentially etched while the α-SiC is stable against the etchants.

In another study (Gabouze et al., 2009), polycrystalline p-type 6H-SiC was etched in a mixture of 22.5 molar hydrofluoric acid and sodium dioxide (Na_2O_2) for 60 minutes at 80 ºC. The etch rate was found to be 230nm/min at 25 ºC at 0 rotation per minute (RPM), the etch depth increases linearly with time. The etching results at this temperature are reported to give a non-uniform etch. At 80 ºC the etch rate increases with temperature then decreases slightly. Also etching at 80 ºC is reported give a uniform and a smooth etched surface.

The Gaseous etching of SiC can be performed using a gas mixture of chlorine trifluoride and nitrogen in the concentration range of 10 –100 % at 800 – 1100 ºC (Habuka et al., 2006). Molten salts mixture such as potassium hydroxide and sodium hydroxide (KOH-NaOH) in the temperature range 400 to 900 ºC is widely used for revealing defects in silicon carbide materials (Landolt et al., 1984).

(Helary et al., 2008) studied the chemical etching of SiC coating layer of coated particles using a Murakami etching solution. The purpose of this study was to investigate the microstructure of the SiC layer in coated particles prior to irradiation. Murakami etchant consists of potassium ferricyanide (K_3FeCN_6) and potassium hydroxide (KOH) at different concentrations with water as the solvent. The use of this etchant showed that the SiC layer etched was chemically treated for 60 minutes. Other experimental parameters were not discussed in detail.

4.3 Conclusion

The chemical and mechanical properties of the particle coatings are an advantage for irradiation purposes. However, when they need to be removed they present major problems. In chapter 3 the chemical properties of coating layers were discussed.

The individual removal of these layers is considered difficult regardless of the method employed. Silicon carbide has been identified as a ceramic that can be attacked chemically with fluorine-based chemicals and gases. It has been shown that this material responds very differently to chemical attack by acids.

The available information on carbon dissolution mostly deals with graphite. The literature shows that the PyC material used for particle coatings can be etched with nitric acid and sulphuric acid. Oxidation of carbon layers at 600 ^{0}C has been found to be effective. However, it is not certain if FPs can be determined from the residue or off gases.

CHAPTER 5

ANALYTICAL TECHNIQUES

Micro-structural and surface features of the coated particle materials and any other changes occurring because of chemical etching were investigated with the following basic experimental characterization techniques.

- Optical Microscopy
- Scanning Electron Microscopy
- SEM equipped with Energy-Dispersive X-ray
- X-Ray Diffraction

5.1 OPTICAL LIGHT MICROSCOPY

Optical microscopy, using a NIKON SMZ800, was the first technique used for simple and fast surface analysis of the samples. The technique uses visible light and a system of lenses to form a magnified real image of the object under investigation. The microscope helps to reveal micro-structural surface features such as grain size, shape and orientation at low magnifications and much lower resolution.

The microscope is equipped with an analysis software package which is used for the digital image acquisition and image processing; the program also offers the option to perform dimensional measurements of the sample.

5.2 SCANNING ELECTRON MICROSCOPE (SEM)

Scanning electron microscopy consists of a versatile non-destructive technique that reveals detailed information about the microstructure, size, shape and other properties of the solid materials investigated. The technique relies upon a beam of high-energy electrons scanned across the surface of the sample to generate a signal. The signal(s) generated from interaction of electrons with the sample contain detailed information about the sample.

Examination of the sample can yield the following information:

- Morphology: the shape, size and arrangement of the particles
- Topography: the texture of the materials

Characteristics of a SEM are high resolution, high magnification and greater depth of field. Magnification that can be obtained with a Zeiss Gemini Ultra Plus Field Emission Gun (FEG) SEM at the university of Pretoria is between 10 and 100 000 X with a resolution of 1 nanometres (Botha, 2009).

When a high-energy electron beam strikes the sample surface, a large number of signals are produced. These signals include secondary electrons (SE), backscattered electrons (BSE) and characteristic X-rays etc., (Figure 18).

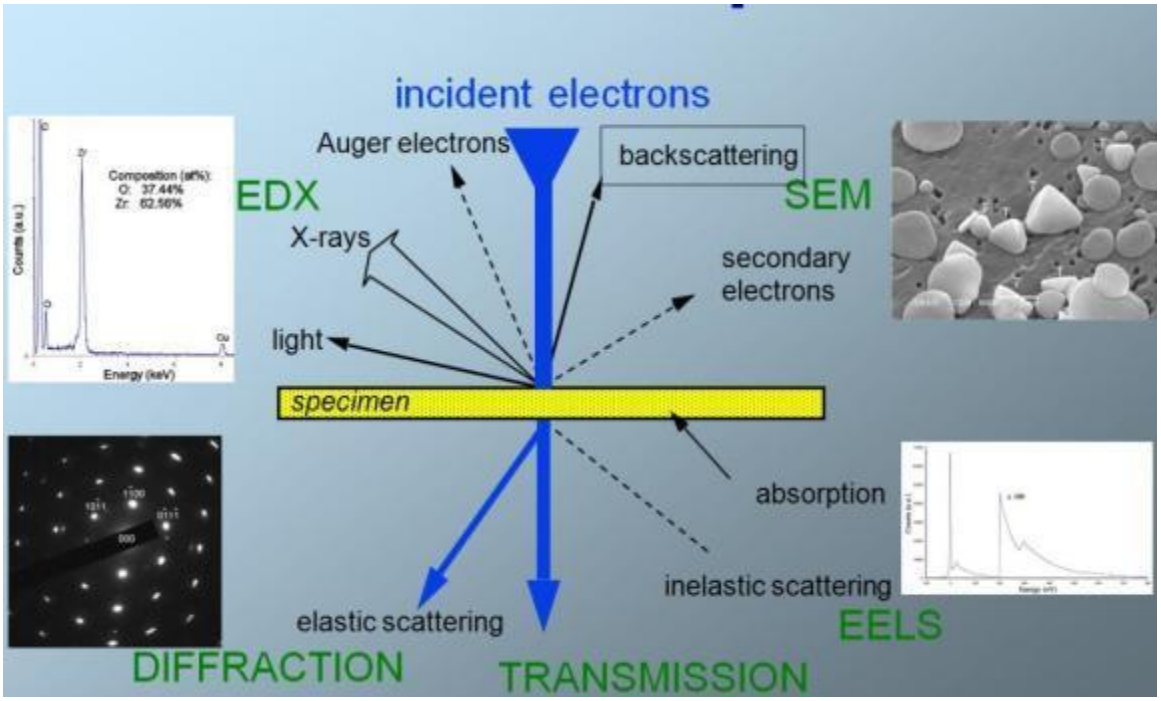

Figure 18: Schematic diagram of signals produced by electron sample interactions during SEM operation (Klopper et al., 2010).

Secondary electrons (SE) and backscattered electron signals are commonly used for imaging samples. SE signals arise from interactions of the electron beam with atoms near the surface of the sample and they have low energy usually 50 eV (Reimer, 1998). These secondary electrons give high-resolution images of surface topography morphology and reveals details about 1 to 5 nm in size.

BSE signals are of high energy, produced by the elastic collisions between the nucleus of the target atom (sample) and the incident electron beam. A BSE signal is a function of atomic weight. The higher the atomic number of the sample the more back scattered electrons are emitted.

5.3 ENERGY DISPERSIVE X-RAY (EDS) ANALYSIS

An energy dispersive X-ray spectrometer is a non-destructive analytical technique used for chemical characterization of materials. It is used in conjunction with a scanning electron microscope to allow chemical information to be collected about the sample under investigation.

When a high-energy beam of electrons from a SEM bombards the sample under investigation, electrons are excited and then ejected from surface atoms of the sample creating an electron vacancy. The resulting vacancies are filled by an electron from a higher energy outer orbital. This event is accompanied by the release of an X-rays photon, characteristic of the element in question.

The EDS detector works by measuring and collecting the number of emitted X-rays and then processing them through a detector system. The information is passed on to a computer system and displayed as a spectrum of energy peaks corresponding to the various elements in the material.

The EDS has a detection limit: Low atomic number elements such as hydrogen and helium etc., cannot be detected due to absorption of low energy X-rays by the detector vacuum window (Klopper et al., 2010).

5.4 X-RAY DIFFRACTION

X-rays, like light, are electromagnetic photons occupying the high-energy upper region of the electromagnetic spectrum between ultraviolet and gamma rays. Compared to light, their wavelength λ is much shorter, ranging from 0.05 to 0.25 nm, thereby allowing for deeper penetration into a material. Being of the same nature as light, they carry an energy equivalent to $h\nu$, where h is Planck's constant and ν is the frequency. Upon interaction with matter, the beam is also reflected or scattered (Cullity, 1977). The amount by which it is absorbed is dependent on the linear absorption coefficient of the material and its penetration depth, amongst others.

XRD is a materials characterization technique based on the coherent scattering of X-rays by crystalline material. Diffraction of X-rays by a crystal is a natural phenomenon occurring when the wavelength of the incident wave motion is of the same order of magnitude as the repeating distance between scattering centres. When a monochromatic beam of X-rays impinges on a crystalline material, it gets scattered in all directions by the atoms/molecules, constituting scattering centres, of the material. The scattered rays may interfere with one another either constructively or destructively depending on their relative phase difference. Constructive interference of such scattered rays results in diffracted beams being produced at specific angles given by Bragg's law, mathematically expressed as:

$$n\lambda = 2d\sin\theta \tag{5.1}$$

Here λ is the wavelength of the incident radiation, d the spacing between diffracting atomic planes and θ the incidence angle. Constructive interference happens when Bragg's equation (1) is satisfied, that is, when the path difference between interfering X-rays is equal to an integral number *n* times wavelength of the radiation. On the contrary, there will be no diffraction in cases where destructive interference occurs. Peaks at specific positions therefore characterize a typical diffraction pattern with a corresponding intensity. The intensity of the scattered beam depends on its direction whilst the peak positions depend on the crystal lattice.

Being non-destructive, the technique can be employed as a tool for identification of phase and crystallographic structure of the material(s). In X-ray diffraction, the material investigated is irradiated with a beam of X-rays to probe spatial and structural arrangements of atoms and molecules to give information about their crystallographic nature. The d spacing is directly related to peak position produced in an X-ray diffraction pattern. The diffraction patterns of single crystal samples orientated at different angles is used to solve the crystal structure of an unknown material.

CHAPTER 6

EXPERIMENTAL METHODS

6.1 INTRODUCTION

This chapter describes the experimental detail of the studies carried out on the controlled removal of the coating layers from coated zirconia particles by means of chemical etching with acidic solutions. The study focused on the outermost layers of the particle namely the outer pyrolytic carbon and silicon carbide layers. A detailed description of method and materials used in the study is provided in the sections below.

6.2 REAGENTS USED

Chemically pure grade 65% wt nitric acid, 98% wt sulfuric acid, 40% wt hydrofluoric acid, ammonium fluoride and perchloric acid, all obtained from Merck and chromium trioxide. Different mixtures were prepared using the above mentioned chemicals, details obtained from Buzelli & Mosen (1977), Fukuda & Iwamoto (1977), Hunter et al. (1990) and Pierson (1993).

6.3 SAMPLES

The samples used in this study were coated simulated fuel particles, manufactured and supplied by PBMR fuel development laboratories at Necsa, Pelindaba. Each particle consists of a ZrO_2 kernel coated first with a porous carbon buffer, then an inner pyrolytic carbon layer, then a silicon carbide layer and finally an outer pyrolytic carbon layer. The coatings were produced by the same chemical vapour deposition process normally used for the production of HTR particles. Exact preparation conditions were not the same for the ZrO_2 kernels; these were altered so that the kernels experience the same fluidizing conditions and temperatures of deposition as in the production of HTR particles. The SEM observed structure and appearance seemed to be the same as for UO_2 coated particles used for fuel Barry (2008).

The diameter of the kernel is about 500 µm and the overall diameter of the coated particle about 1 mm. The thickness for each coating layer ranged from 35 to 95 µm. Other characteristics of the particle are displayed in Table 2 (Barry, 2008)

Table 2: Characteristics of a simulated coated particle

TRISO Coated Particle Characteristics and Nominal Layer Thicknesses (µm)	
Kernel composition	Zirconia dioxide (ZrO_2)
Kernel diameter (µm)	± 500
Porous buffer layer	95 ± 18
Inner pyrolytic carbon	40 ± 10
Silicon carbide	35 ± 4
Outer pyrolytic carbon	40 ± 10

A typical scanning electron microscope image of transverse section of a zirconia TRISO coated particle illustrating the various layers is shown in Figure 19.

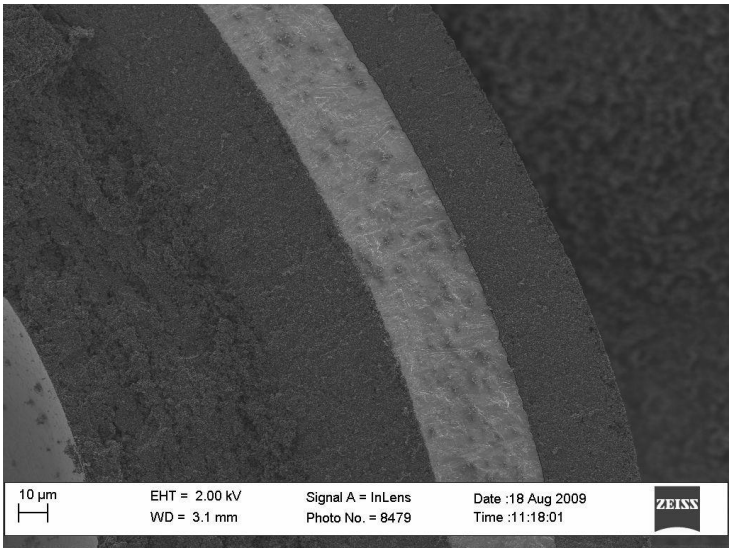

Figure 19: SEM image of a simulated TRISO coated particle

6.3.1 Determination of Particle Size

The diameter of approximately 150 particles were measured before etching, using a pair of digital callipers as well as a NIKON optical stereo microscope equipped with digital software. Each of these particles were measured 6 times to obtain a reliable average for the diameter. The distribution of particle diameters is presented in Figure 20. The error for each average is roughly ± 0.01 mm, thus there is a slight deviation from sphericity. The exact reason for the distribution appearing to be the superposition of three normal distributions, is not possible to determine without recourse to the production history of the exact batches received form PBMR. This was not possible at the time of writing.

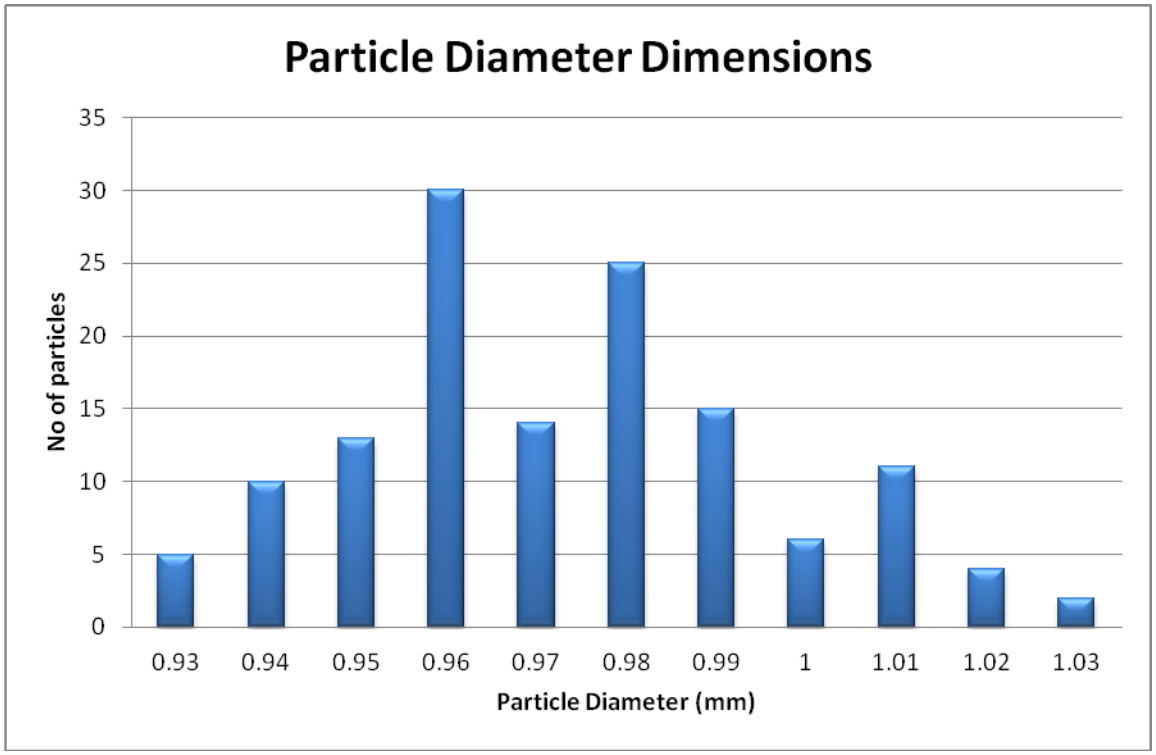

Figure 20: Distribution of the diameter values for TRISO particles

From the distribution (Figure 20) 20 particles with diameters between 0.94 to 0.99 mm diameters were selected for treatment, as discussed later in Section 7.1.3.

6.4 CHEMICAL ETCHING OF PYROLYTIC CARBON LAYER

6.4.1 Apparatus

A reflux condenser system and hot plate were employed to study the chemical dissolution of carbon layers. The reflux technique is often used in chemistry to supply heat for a chemical reaction in a closed system. Typical reflux apparatus includes a vessel with liquid mixture which is placed in a heating mantle and is connected to a condenser. The condenser is water cooled through circulating cold water which enters from the bottom opening and escapes through the top opening. Water circulation was maintained by a pump placed in a tub containing cold water. A schematic diagram of the reflux system is shown in Figure 21.

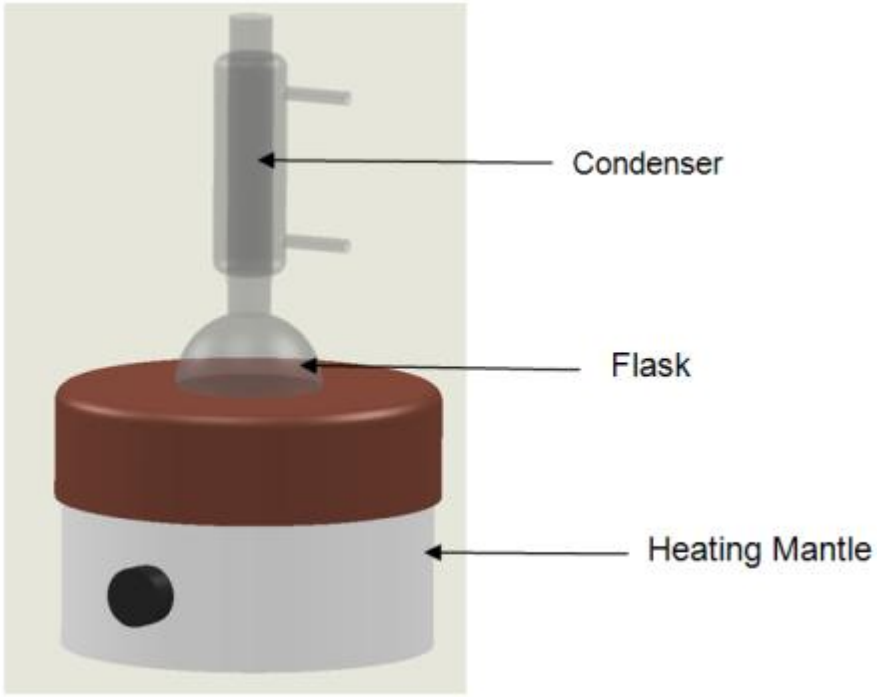

Figure 21: Schematic of the reflux condenser system used.

6.4.2 Experimental Procedure

Three etching reagents were prepared as follows: (i) H_2SO_4 and HNO_3 (3-5 ml of each in a 1:1 ratio); (ii) a mixture of H_2SO_4 (6 ml), HNO_3 (6 ml) and HClO4 (10 ml); and (iii) 10 ml HNO_3 plus 15 ml H_2SO_4 to which 2 to 2.5 g of CrO_3 was added. The composition, volume and details of each prepared mixture are presented in Table 3. The information on the mixtures used in the present work were obtained from literature (Buzelli & Mosen (1977) and Pierson (1993)).

Table 3: Chemical etchants used for OPyC layer

Reagent	Components	Volume (ml)
1		
	HNO_3	10
	H_2SO_4	10
	$HClO_4$	5
2	HNO_3	10
	H_2SO_4	10
3	H_2SO_4	6
	HNO_3	3
	CrO_3	2 gram

6.4.2.1 Etching using a Hot Plate

Experiments were carried out separately using the prepared solution described in Table 3. In each experiment the pre-weighed sample, about 0.5 g of coated particles, was added to the glass beaker. To this about 15 ml of the solution from the prepared mixture (using either reagent 1 or 2 or 3) was added. After introduction of the particle and reagent, the beaker was placed on a hot plate and heated at temperatures of 100 ºC up to 145 ºC for 10-60 minutes or until suitable results were attained.

After etching, the beaker is allowed to cool and the solution is diluted with 15 ml deionised water. The samples were filtered carefully, transferred to an empty beaker and rinsed thoroughly with deionised water and acetone. The retrieved samples were

dried at 60 ºC for about 1.5 hours. Upon the completion of etching and washing the particle diameters were determine using the same procedure described in Section 6.3.1. The optical examination of the particle's surface was then performed with an optical microscope and a SEM. In some cases the etching process was repeated with a fresh etching solution until satisfactory results were obtained.

6.4.2.2 Etching Using a Reflux System

The same method described in Section 6.3.4.1 was followed, but the reaction was carried out in the reflux system. In these experiments a condenser was attached to the flask containing samples and placed on the heating mantle. The condenser is water cooled through circulating cold water which enters from the bottom opening and escapes through the top opening. Constant water circulation was maintained by means of a pump placed in cold water.

6.5 CHEMICAL ETCHING OF SILICON CARBIDE LAYER

6.5.1 Samples

To investigate the chemical etching of the silicon carbide layer the samples used were particles consisted of zirconia kernels which where only coated up to the silicon carbide layer; that is without any application of the outer pyrolytic carbon layer. The other particle characteristics were the same as in Section 6.3.

6.5.2 Apparatus

Chemical etching of the silicon carbide layer was carried out using two main techniques: a MARS 5 programmable microwave digestion unit with a power setting of 500 W at a frequency of 2450 MHz and heating in a muffle furnace.

6.5.3 Experimental procedure

6.5.3.1 Dissolution in a Muffle Furnace

Initial experiments were carried out to determine which conditions might produce complete dissolution of the layer. In each case, a sample weighing between 0.5 to 1.0 g

was introduced into a Teflon beaker and the prepared mixture or reagent ~ 6 ml was added. Experimental conditions are presented in Table 4.The vessels were closed tightly and inserted in the furnace. The temperature was set between 300 to 350 ºC and the reaction was carried for about 5 hours. Thereafter the beakers were allowed to cool and the solution diluted with ~ 50 ml deionised water. Samples were dried at 60 ºC and observed under the microscope.

Table 4: Acid composition, concentration and volume used in etching of SiC layer

Reagent	Components	Volume (ml)
1	HF	8
2	HF	10
	HNO_3	10
	H_2SO_4	10
3	HF	3
	HNO_3	3
3	NH4F.HF	8

6.5.3.2 Dissolution in a Microwave Digester

The same reagents and sample size described in Section 6.5.3.1 were used. Samples were transferred to microwave reaction vessels. To each vessel 6-8 ml of the different reagent was used. The vessels were then closed and capped tightly in accordance with the manufacturer's guidelines and placed in the microwave oven. The heating system consisted of a three stage power setting with pre-set temperature and pressure. The heating program starts with a 10 minute cycle where the temperature is ramped to 200 ºC and held for 60 minutes. After elapse of the holding time a cooling step is applied for 10 minutes until 60 ºC is reached.

The vessels were then removed from the MARS and cooled for a further 15 minutes. When cooled, they were uncapped and the solution diluted with distilled water (~20 ml),

and the retrieved samples were washed extensively using de-ionised water (30 ml) and then dried at 60 ºC for approximately 1.5 hours.

A surface examination was conducted on these etched samples and when applicable some were etched again using a fresh solution every 60 minutes for up to 3 hours.

6.6 INSTRUMENTS USED TO ANALYSE RESULTS

6.6.1 Optical Light Microscope

Imaging of the sample materials in the as-received condition as well as samples treated with chemical etchants was carried out with the Nikon SMZ 800 optical stereo microscope equipped with a computerised digital camera (Olympus image analysis software). This system allows capturing of images and the option to measure the size of the samples. The samples were examined using different magnifications up to 50 times. Examination of sample surfaces with this technique was not very helpful compared to SEM imaging, since this technique only shows morphological features such as size and shape and very little detail concerning the microstructure of the samples.

6.6.2 Scanning Electron Microscope (SEM)

Imaging and detailed investigations of the samples at high magnifications were accomplished using a ZEISS ULTRA PLUS Field Emission Scanning Electron Microscope (at the University of Pretoria, Laboratory for Microscopy and Microanalysis). The purpose of the SEM examination was to determine what morphological and microstructural changes occur when the layers are chemically treated. Examination was carried out on samples before and after chemical etching. SEM samples were prepared by mounting the relevant samples on an aluminium holder using conductive carbon tape which prevents the samples from moving during handling and eliminates the need for sputter coating. The holder was then placed on the motorized stage, for quick and simple sample navigation, located in the specimen chamber. The instrument was operated under high vacuum at an accelerating voltage of 2 kV at all times (since this was done by an independent party, there was not no room to improve or adjust this at

the time) . The sample surface was mainly characterized using the secondary electron detector.

6.6.3 Energy Dispersive X-ray

Chemical analysis of the samples was carried out using a SEM model FEI Quanta 200 3D, equipped with an energy dispersive spectroscopy (EDS) system at the Nuclear Energy Corporation of South Africa (Necsa). EDS is an X-ray technique used to identify the elemental composition of a sample. SEM sample preparation procedures are applicable for EDS-analysis.

Samples to be investigated were placed inside the specimen chamber and the samples were exposed to an electron beam. Digital imaging was used to identify areas of interest on the sample and chemical analysis could be determined for more than one feature. The resulting analysis provides element identification and concentration.

6.6.4 X-Ray Diffraction

X-ray diffraction (XRD) measurements were performed on silicon carbide layers for chemical phase identification. The technique was employed in conjunction with 2007 PDF-2 database.

CHAPTER 7

RESULTS AND DISCUSSIONS

7.1 ETCHING OF OUTER PYROLYTIC CARBON LAYER

7.1.1 Etching Method

In these experiments the reactions carried out using a hot plate were found to have some limitations. It was observed that after heating at 120 to 140 ºC for more than 15 minutes the acid mixture evaporates and changes the concentration. The mixture became lumpy making it difficult to extract the samples for further analysis. At this stage it was decided to make use of the reflux system.

The method of heating using the reflux method as described in (Buzelli & Mosen, 1976) was used alternatively to investigate etching of the OPyC layer. The reaction carried out under the reflux system provided more favourable results compared to heating using the hot plate. Using the reflux system, the reaction was performed for an extended period of time without loss of etchant and change in concentration. Another advantage is that if the system is used in hot cells it can minimize corrosion due to enclosed corrosive gases. However, during the experiments, the released vapours were not analysed.

7.1.2 Dissolution of the OPyC Layer in Various Mixtures

- **Dissolution in HNO_3/H_2SO_4-$HClO_4$:** The reactions carried out with the first reagent, a mixture of concentrated HNO_3:H_2SO_4:$HClO_4$, were performed up to temperatures of 80 ºC for 1 hour. Nitric acid and perchloric acid were both used because of their strong oxidising properties. Dissolution of the layer was not observed at all using this mixture at temperatures of about 80 ºC. It was decided to stop this reaction after 1 hour of etching due to fumes that were released during heating. In addition perchloric acid is a potential explosion hazard (Buzelli & Mosen, 1977). This solution was therefore considered unsafe to use at temperatures above 100 ºC.

- **Dissolution in HNO_3/H_2SO_4:** In the literature (Bokros, 1969), it was demonstrated that a nitric and sulfuric acid mixture is a strongly oxidising medium in which carbon and other organic materials are known to dissolve. This mixture was used under various experimental conditions at low (60 ºC) temperatures and high temperatures (140 ºC) with varying amounts of nitric and sulfuric acids. The study revealed that the pyrolytic carbon was unchanged in this mixture. Microscopic examination of sample surfaces treated with this etchant solution did not show any structural changes or removal of the layer even when the solution was heated for a long time.
- **Dissolution in CrO_3-HNO_3/H_2SO_4:** Among the three dissolution mixtures used in this study, the CrO_3-HNO_3/H_2SO_4 solution provided the best results. Particles etched in this solution at 120 to 140 ºC for 10 to 35 minutes were observed to have a grey metallic surface. The chemical reaction with the solution CrO_3-HNO_3/H_2SO_4 was investigated in detail a single simulated coated particle to find out the best etching conditions. Parameters tabulated in Table 5 were identified as the favourable conditions for etching OPyC layer from single coated particle.

Table 5: Identified etching conditions of OPyC for a single coated particle

Experimental Conditions for OPyC dissolution		
Acid	Concentration	Volume
Nitric (HNO_3)	14 Molar	3 ml
Sulfuric (H_2SO_4)	18 Molar	3 ml
Chromic oxide (CrO_3)		0.5 g
Etching Temperature: 130 – 140 ^{0}C		
Etching Time: 10 to 15 minutes (for a single coated particle)		

In this reaction three oxidants are present. The reactions of nitric and sulfuric acids were mentioned in paragraph 3.3.3.1. The chemistry of CrO_3 is as follows (Cotton and Wilkinson, 1980). It dissolves in water and equilibrates into the dichromate anion and protons as follows:

$$2CrO_{3\,(s)} + H_2O_{(l)} \rightarrow Cr_2O_7^{2-}{}_{(aq)} + 2H^+{}_{(aq)} \qquad (7.1)$$

In the presence of additional protons, e.g. from the two mineral acids present, the oxidation of carbon by the dichromate anion proceeds as follows:

$$2Cr_2O_7^{2-}{}_{(aq)} + 16H^+{}_{(aq)} + 3C_{(s)} \rightarrow 4Cr3^+{}_{(aq)} + 8H_2O_{(l)} + 3CO_{2\,(g)} \qquad (7.2)$$

7.1.3 Determining the Thickness of the Layer Removed

The sample size for the removal of the OPyC layer consisted of 30 selected coated particles, with diameters between 0.94 and 0.99 mm, where every particle was measured 6 times to obtain a mean particle diameter. Appendix A, provides diameter measurement for selected particles before etching. The data indicates that the individual diameter measurement results obtained for each particle varies from 10 to 30 microns. The possible factors that could have contributed to these variations include the particle shapes, the coated particles are not perfectly spherical each measurement could result from a different orientation of the particle. The accuracy of the measurements can be improved by the use of automated devices such as automated optical microscopy and particle size analyser (PSA) (Kercher et al., 2008). These devices allow a large sample size and automated measurements instead of a handful of manual measurements. The devices where not available to our department due to limited resources.

The data set measurements for each particle were averaged out; Figure 22 displays the distribution attained. The distribution shows the data is spread out from 0.94 to 0.99 mm with 60% of particles in the range of 0.97 mm and 0.98 mm. About 6 particles displayed a diameter less than 0.97 mm and 5 particles were greater than 0.98 mm. The data set for each particle was used to compute descriptive statistics mean diameter, which was found to be 0.97 mm. The resulting distribution is not a good or normal distribution, it is

vital to recall that the samples used for the study were selected only from the range 0.94 to 0.98 mm. The calculated standard deviation from the mean was found to be 0.010 mm, it indicates that the diameter values for the data are tightly close to mean.

Bin	Frequency
0.96	6
0.97	8
0.98	11
0.99	5

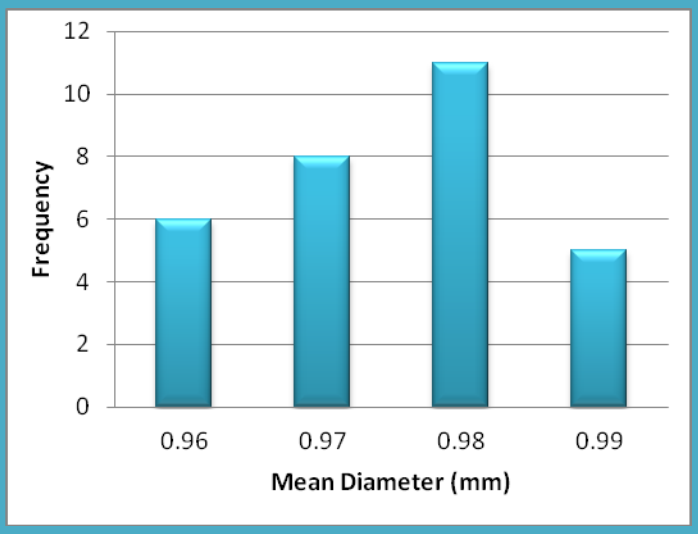

Figure 22: Distribution obtained through mean diameter measurements

After etching particles were chosen randomly to measure the final diameter, using the same method described in Section 7.1.3. Appendix B, provides measurement for each coated particle after etching. From the data, the distribution of mean particle diameter for particle data set obtained (Figure 23), indicates that a large number of particles are centred in the range 0.86 to 0.87 mm. The calculated mean diameter is 0.87 mm with a standard deviation of 0.0141 mm.

Bin	Frequency
0.85	5
0.86	8
0.87	8
0.88	4
0.89	3
0.9	2

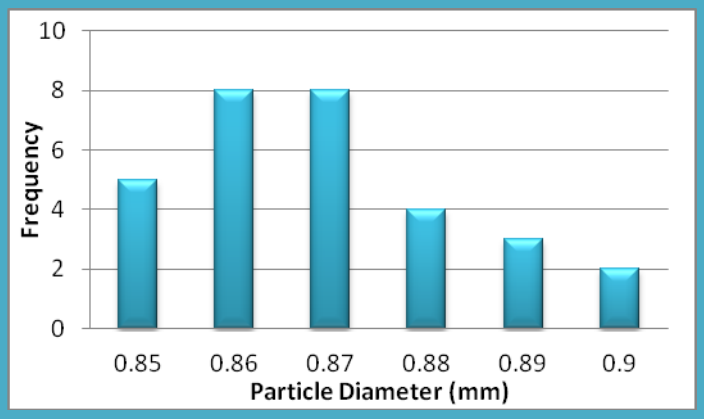

Figure 23: Distribution obtained through mean diameter measurements

The descriptive statistics of the data was computed using the following calculations

$$\bar{x} = \frac{1}{N}\sum_{i=1}^{N} x_i \quad \text{(Mean)} \quad (7.3)$$

$$\sigma^2 = \frac{1}{N-1}\sum_{i=1}^{N}(x_i - x)^2 \quad \text{(Variance)} \quad (7.4)$$

$$S = \sqrt{\sigma^2} \quad \text{(Standard deviation)} \quad (7.5)$$

$$\Delta R = R_{Initial} - R_{final} = \left(\frac{\overline{D_i} - \overline{D_f}}{2}\right) \quad \text{(Layer thickness removed)} \quad (7.6)$$

Descriptions

- Equation 7.3: the mean is the sum of the values in a sample divided by the number of values.
- Equation 7.4: the variance is calculated as the average squared deviation from the mean.
- Equation 7.5: the standard deviation is the square root measure of the variance; it is a measure of how widely values are dispersed from average value.

- Equation 7.6: The equation was used to calculate the thickness of the layer removed (R), R represents the radius of the particle; D_i and D_f are the mean values of coated particle diameters before and after etching. The formula assumes that the particles are spherical in shape.

Table 6: Descriptive statistics for CP diameter values

Attribute	N	Min (mm)	Max (mm)	Mean (mm)	Standard deviation for the data set (mm)
Value before etching	30	0.94	0.99	0.96	0.009
Value after etching	30	0.84	0.90	0.87	0.014
Thickness removed: $\Delta R = R_{Initial} - R_{final} = \left(\frac{\overline{D_i} - \overline{D_f}}{2}\right) = \left(\frac{0.96-0.87}{2}\right) = 0.05\ mm$					

Using equation 7.6 the thickness of the layer removed is 0.05 mm (see Table 6). Looking at the PBMR nominal value for the OPyC layer Table 7, the thickness falls in the range of 40 ± 10 µm (0.04 ± 0.01). The calculated value from our experimental work is found to be within limits.

Table 7: PBMR nominal values (Barry, 2008)

Parameter	Value (mm)
Average particle diameter	0.92
OPyC layer thickness	0.04 ± 0.01

7.1.4 Determining the Removal/Etch Rate

The kinetics of the etching rate was studied as a function of change in diameter over change in time at constant temperature (130-140 ºC). The data was taken from three coated particles etched separately in 10 ml of CrO_3-HNO_3/H_2SO_4 solution in a 5 ml

beaker, at temperature of 130 to 140 ºC. In each case the particle was etched for 1 minute, cooled, washed and measured, followed by further etching. The heating method used in this case was the hot plate; the heating temperature was measured directly by the thermometer. Figure 24 shows the particle diameter as a function of time, for the three particles. The reaction appears to start after an induction time of 6-10 minutes of heating.

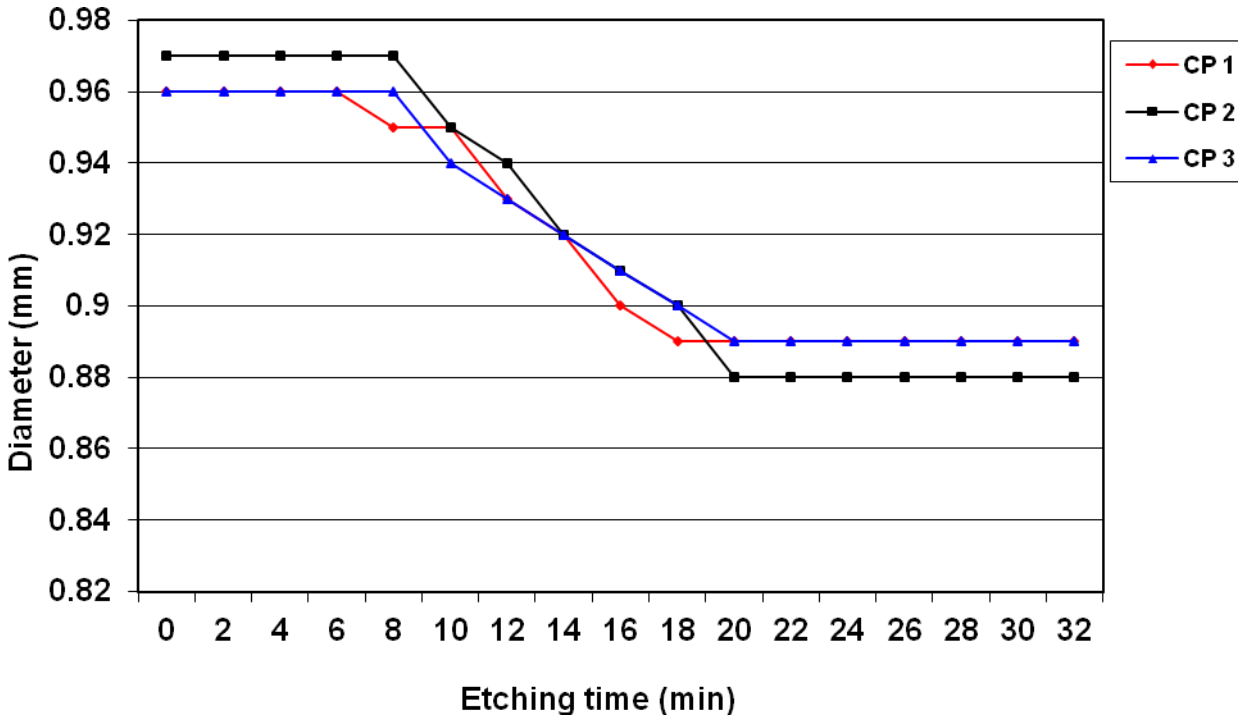

Figure 24: Etching of OPyC in the CrO_3-HNO_3/H_2SO_4 solution

Coated Particle 1

$$\Delta x = \frac{\Delta\, diameter}{\Delta\, time} = \frac{0.95-0.9}{18-8} = 0.005\ mm/min$$

Coated Particle 2

$$\Delta x = \frac{\Delta\, diameter}{\Delta\, time} = \frac{0.97-0.9}{19-9} = 0.007\ mm/min$$

Coated Particle 3

$$\Delta x = \frac{\Delta\, diameter}{\Delta\, time} = \frac{0.94-0.9}{17-11} = 0.006\ mm/min$$

The removal rate defined by change in diameter over change in time change appears to be linear once the reaction has started, after an induction period, and is 6 ± 1 μm/min.

The linearity can be explained in terms of a simple kinetic model. If it is assumed the reaction rate is proportional to the available surface area, we can write the mass loss rate as:

$$-\frac{dm}{dt} = k4\pi r^2 \qquad (7.7)$$

Here *m* is the mass, *t* is time, *r* is the particle radius, and *k* is the proportionality constant. Since

$$m = \rho\frac{4}{3}\pi r^3 \qquad (7.8)$$

we have

$$dm = \rho 4\pi r^2 dr \qquad (7.9)$$

Here *ρ* is the material density. After substitution of (7.9) into (7.7), appropriate cancelation, and separation of variables, one arrives at:

$$-\int_R^r dr = \frac{k}{\rho}\int_0^t dt \qquad (7.10)$$

After integration this yields the linear rate equation:

$$r = R - \frac{k}{\rho}t \qquad (7.11)$$

R is the starting radius. Using a average density of 1.75 g cm^{-3} the proportionality constant for the etch rate is (1.05 ± 0.02) X 10^{-11} gμm^{-2} min^{-1}. The density value used was supplied by the PBMR group, and is slightly lower than typical literature values found in the literature, e.g. the 2.05 g cm^{-3} for carbon graphite Bokros (1969).

7.1.5 Sample Surface Analysis

7.1.5.1 Optical Microscopy

The surface appearance of coated fuel particles prior and after etching in CrO_3-HNO_3/H_2SO_4 media was examined by optical microscopy. This method enabled a quick comparison of etched and untreated sample features. The outer surface (Figure 25) of particles prior to chemical etching appeared black in colour with an even surface.

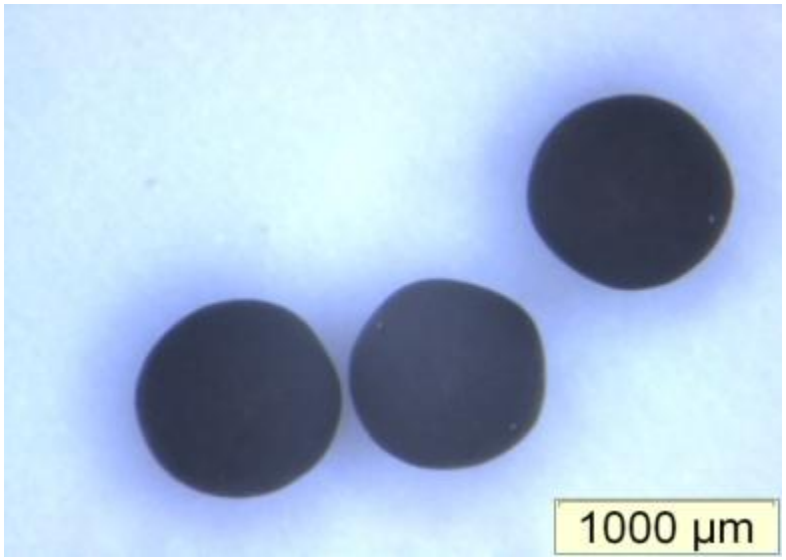

Figure 25: Optical light microscopy of coated particles surface before etching

After chemical etching Figure 26 surfaces appeared later on with uneven metallic grey, shiny texture. This phenomenon could be attributed to the fact that the OPyC layer is completely removed by the chemical treatment to reveal the silicon carbide ceramic layer underneath.

The optical microscope examination of the particle surfaces provided very limited information about micro structural features of the material; hence it was decided to use a scanning electron microscope for a detailed examination.

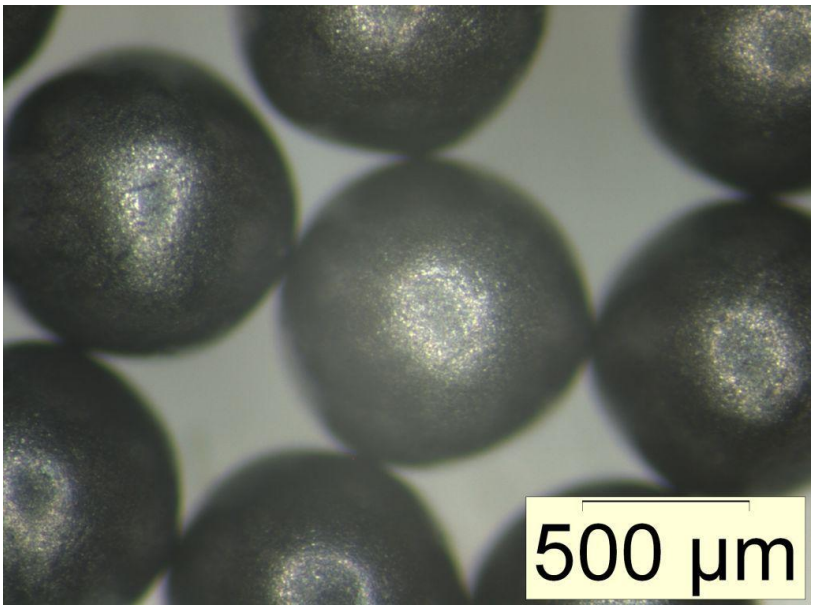

Figure 26: Optical micrograph of particle surfaces after removal of outer carbon layer

7.1.5.2 Scanning Electron Microscope (SEM) Examination

For a more in-depth study of surface morphology and microstructure features of coated particles prior and after chemical etching a ZEIS ULTRA PLUS Field Emission SEM was used. Several samples were examined and representative regions of interest photographed. The OPyC surface prior to chemical etching (Figure 27) shows a closely packed material with globular features and interspatial voids.

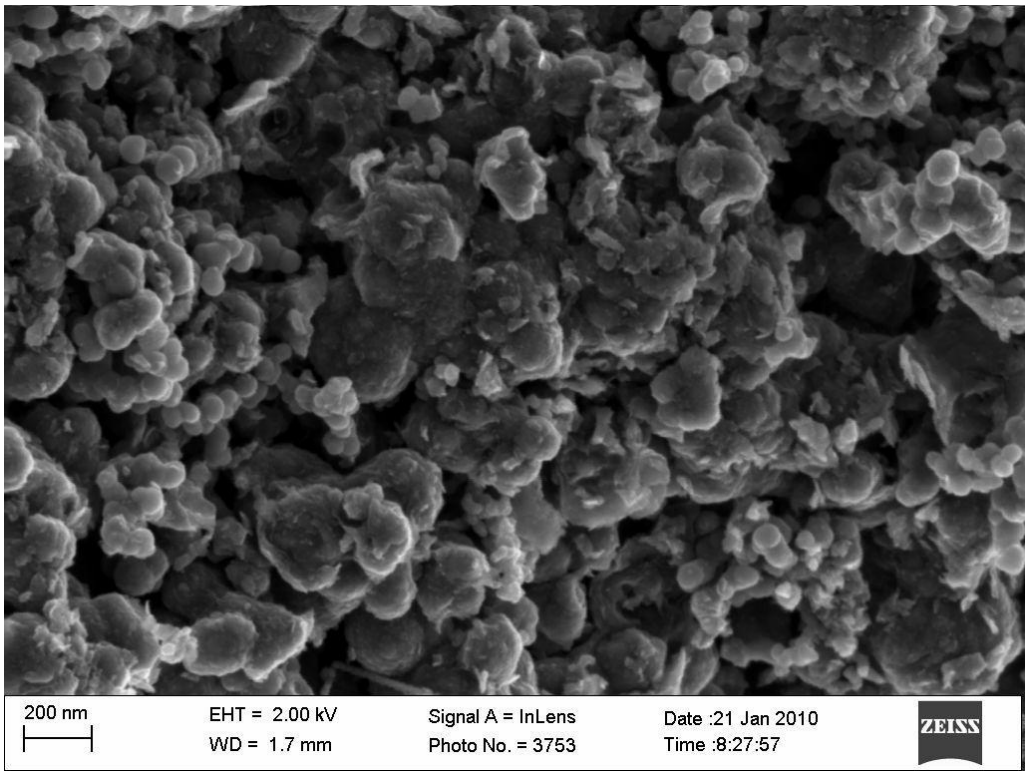

Figure 27: Surface of OPyC prior to chemical treatment.

To investigate how pyrolytic carbon decomposes under the chemical treatment by CrO_3 -HNO_3/H_2SO_4 solution a coated particle sample was partially etched for 10 minutes. SEM examination of the surface Figure 28 reveals a structure which is dominated by better defined globular features and voids that are more prominent and linked together. It is believed that the chemical etchant penetrates between the carbon globules resulting in disintegration of the layer. The examination also implies that there are two sub-structures within the pyrolytic carbon, one which is preferentially removed.

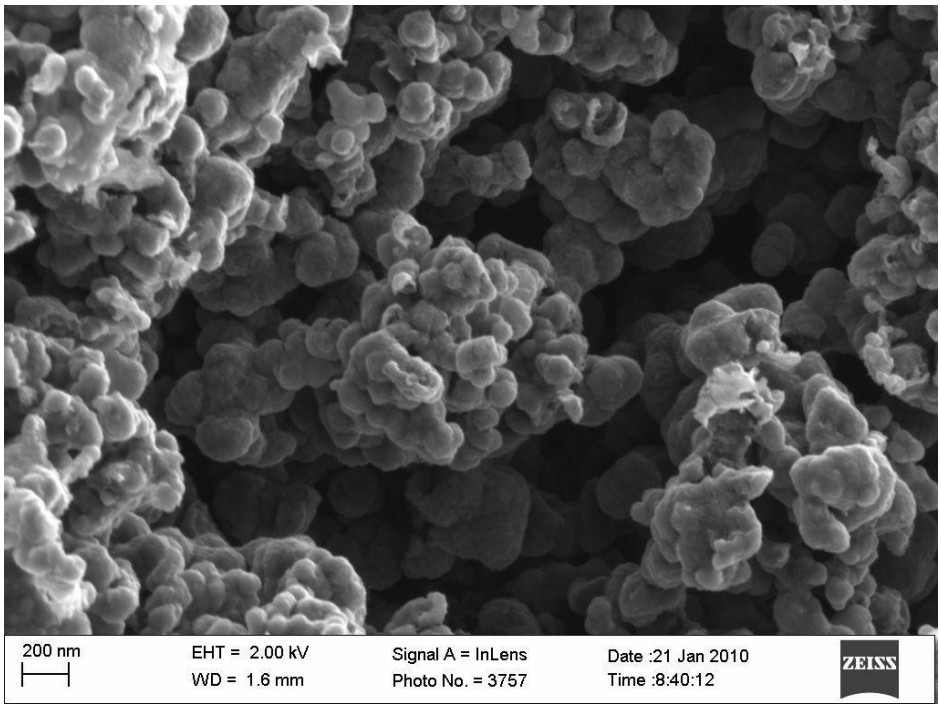

Figure 28: SEM Micrographs of OPyC surface etched for 10 minutes

After completion of the chemical treatment to remove the OPyC layer SEM examinations showed that the globular amorphous features that were visible on the untreated (Figure 27) as well as the partially etched sample (Figure 28), are no longer visible. The microstructure is now dominated by crystalline grains of varying sizes. The presence of band markings in the grains are a feature of a re-crystallised structure and are called twin bands which are regions of changed atomic orientation within the crystal arising from faults in the stacking sequence of the atomic planes. To designate a representative area of the sample, images were taken at a lower magnification than compared to that of the particle surface prior to chemical treatment (Figure 29). The results confirm that the OPyC layer has been completely removed with no indication of physical damage caused by the etching solution to the silicon carbide surface.

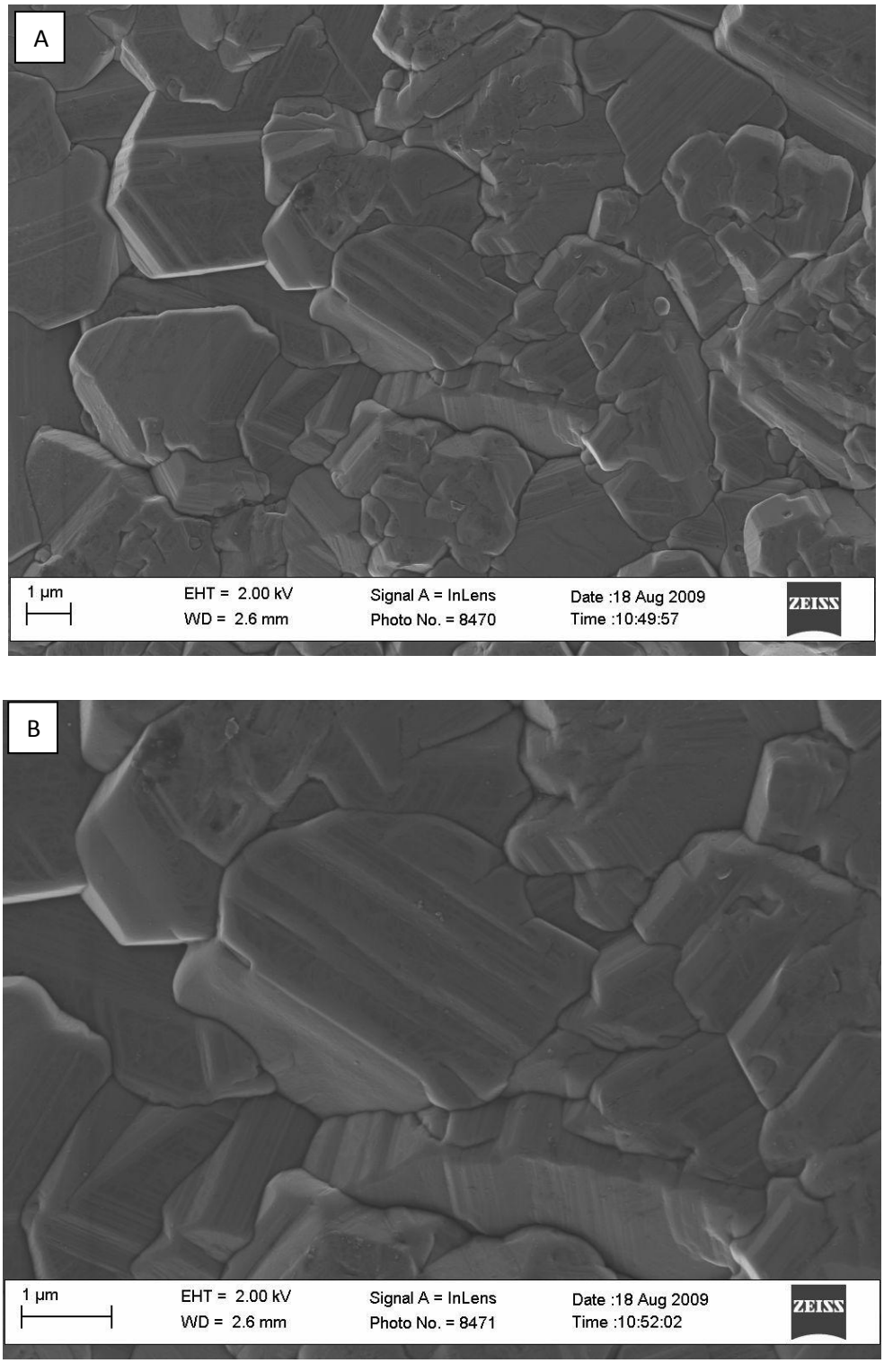

Figure 29: SEM micrographs of SiC surface after removal of OPyC at different magnifications

For comparison, the surface of the particle without application of the OPyC coating (with virgin SiC surface) was examined at the same magnification as that of the particles where the OPyC layer was removed chemically. SEM examination (Figure 30) shows also a microstructure that contains grains.

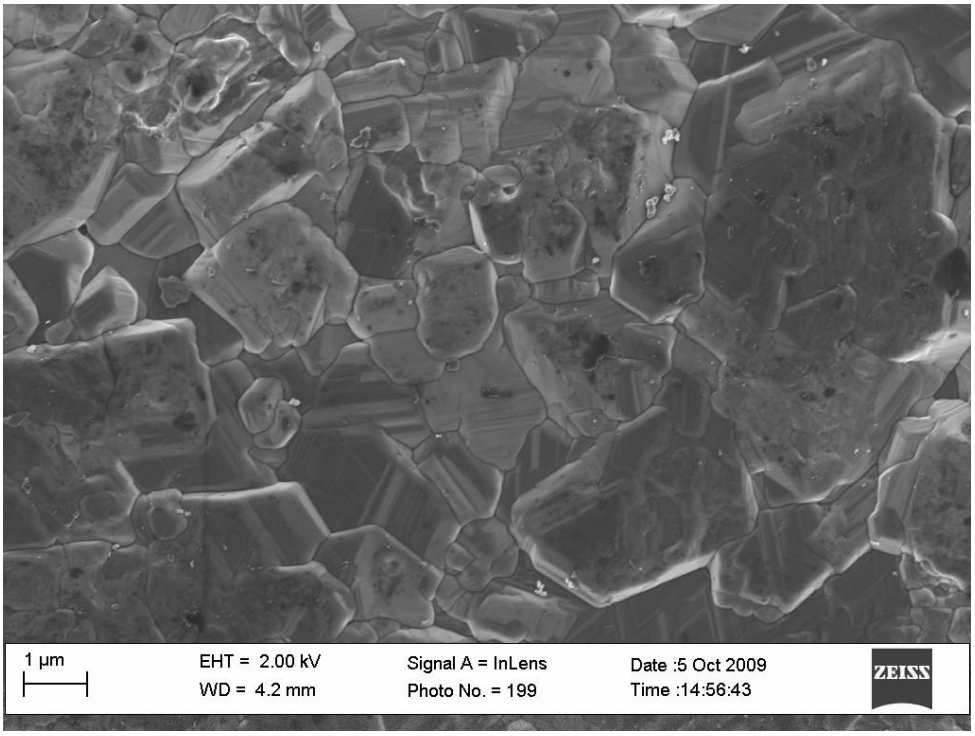

Figure 30: SEM micrographs of virgin SiC

7.1.6 Energy Dispersive X-ray Spectroscopy (EDS) analysis

7.1.6.1 EDS Analysis of Unetched Surface

Energy dispersive X-ray spectroscopic analysis (EDS) was done on the outer surface of the particles before and after chemical etching. The goal of this analysis was to determine if there is any change in elemental surface composition of the samples after etching. Chemical composition of the samples under investigation is one of the parameters that would indicate if the samples have been successfully etched and if the elemental composition of the underlying layer is affected by the acidic solution used.

The EDS spectrum obtained from the untreated outer surface of a particle (Figure 31) reveals that the surface composition consists completely of carbon and correlates with the pyrolytic carbon that is used for the deposition of the outer layer. The quantitative EDS composition in Table 8 verifies that the elemental composition identified in the spectrum consists only of the element carbon.

Table 8: EDS analysis of the Coated Particle outer surface before removal of OPyC layer

EDAX ZAF Quantification (Standardless)
Element Normalized
SEC Table : Default

Element	Wt %	At %	K-Ratio	Z	A	F
C K	100.00	100.00	1.0000	1.0000	1.0000	1.0000
Total	100.00	100.00				

Element	Net Inte.	Bkgd Inte.	Inte. Error	P/B
C K	907.96	1.34	0.47	677.58

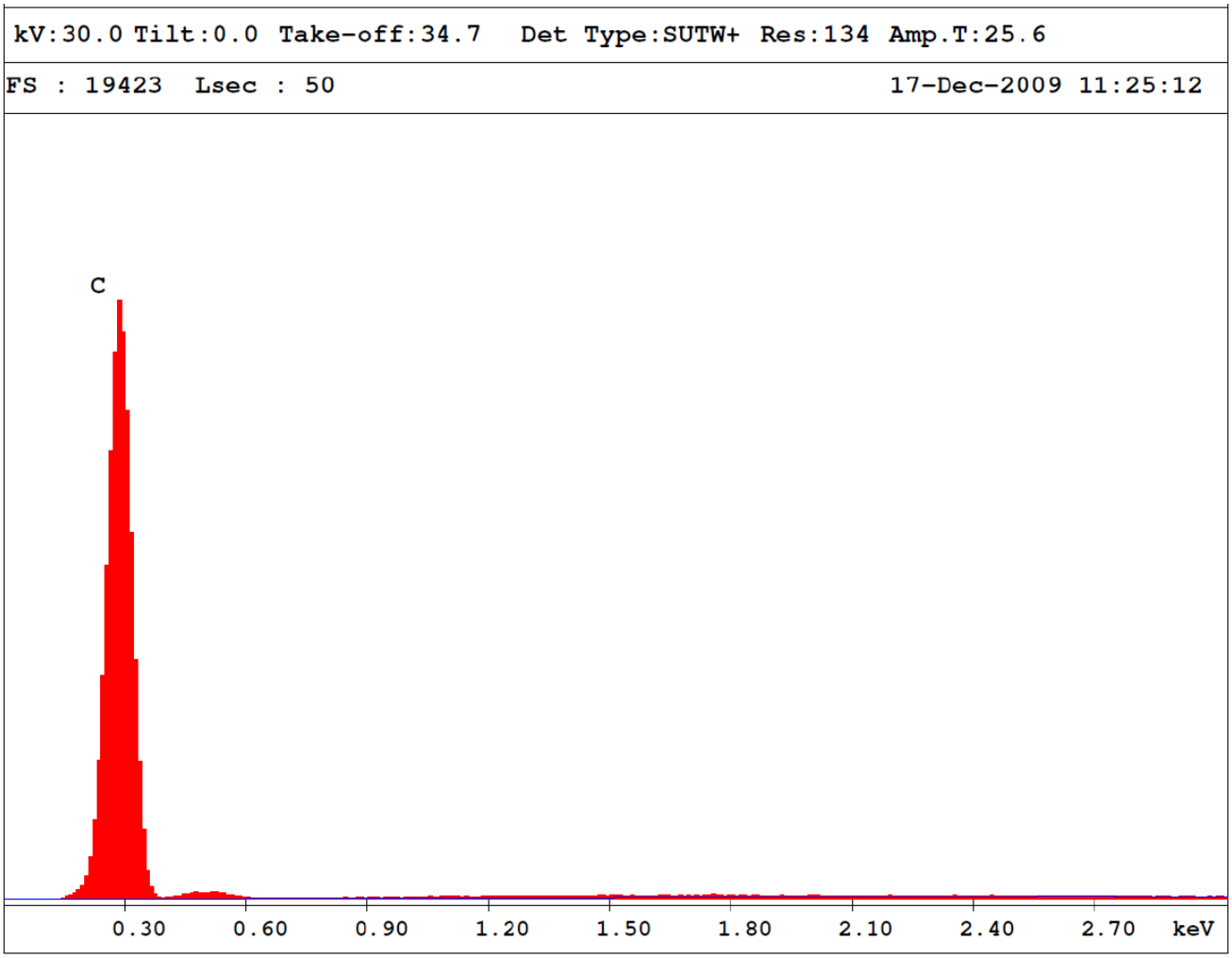

Figure 31: EDS spectrum of CP surface before chemical treatment of the OPyC layer

7.1.6.2 EDS Analysis after Chemical Treatment of the OPyC Layer

Elemental analysis of the CP surface etched in CrO_3 -HNO_3/H_2SO_4 solution indicates the presence of both silicon and carbon (Figure 32). Whenever low atomic number elements are detected in an acquired spectrum, peak heights cannot be compared directly for quantitative information when a high accelerating voltage of 30kV is used. Quantitative analysis is therefore recommended and this result (Table 9) corresponds to the calculated weight percentage of the chemical compound with formula SiC (silicon carbide).

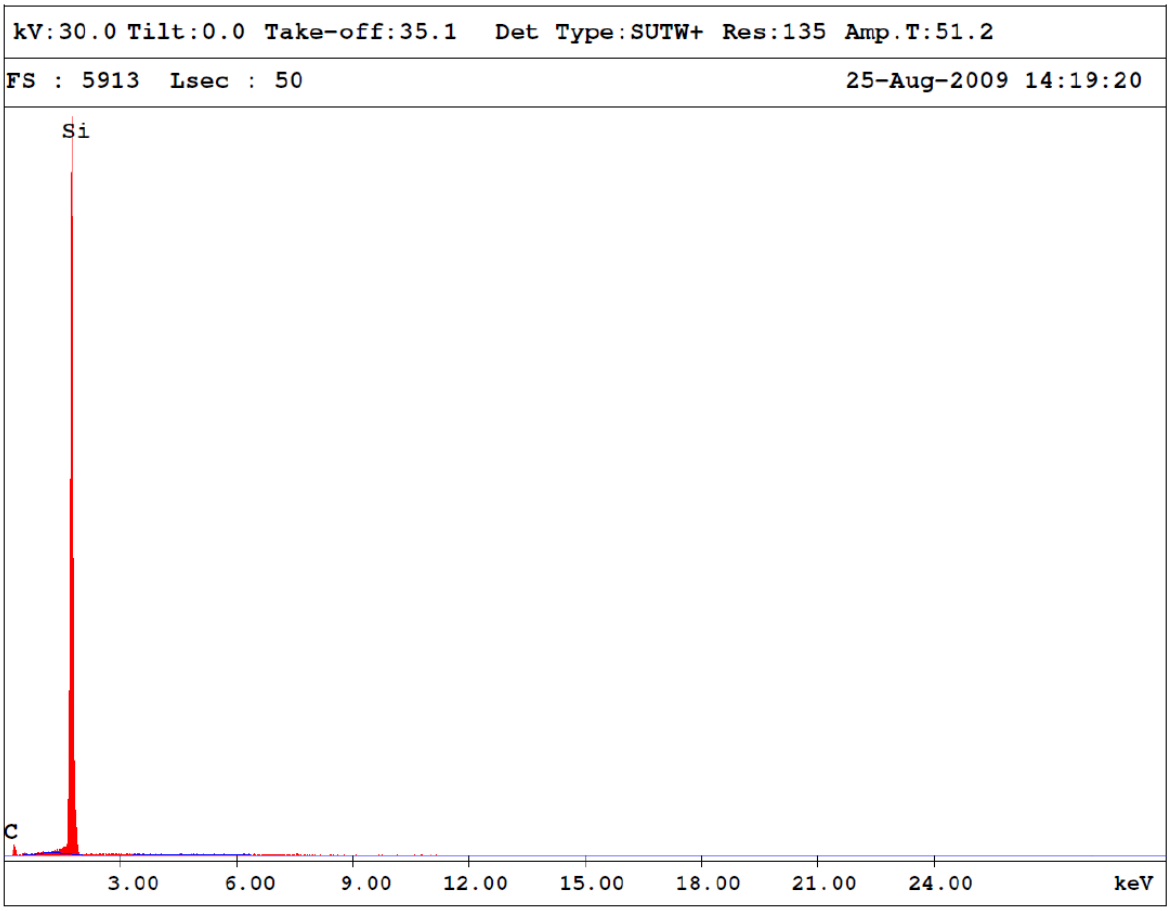

Figure 32: EDS spectrum of CP surface after removal of the OPyC layer

This confirms that the observed surface after chemical etching is silicon carbide. A further conclusion is that the outer pyrolytic carbon layer, previously covering the SiC layer, has been completely removed by the chemical treatment used. The analysis did not reveal that the SiC compound was contaminated by the etchants used to remove the outer carbon layer.

Table 9: EDS Analysis of SiC surface after removal of OPyC layer

EDAX ZAF Quantification (Standardless)
Element Normalized
SEC Table : Default

Element	Wt %	At %	K-Ratio	Z	A	F
C K	30.35	50.47	0.0278	1.0346	0.0887	1.0001
SiK	69.65	49.53	0.6635	0.9843	0.9679	1.0000
Total	100.00	100.00				

Element	Net Inte.	Bkgd Inte.	Inte. Error	P/B
C K	5.06	0.50	6.88	10.12
SiK	830.06	2.58	0.49	321.73

7.2 ETCHING RESULTS OF SILICON CARBIDE LAYER

7.2.1 Silicon Carbide Dissolution

In the literature (Harris, 1995), it was found that silicon carbide is a rigid material which is relatively inert to attack by most aqueous solutions. Dilute or concentrated HF acid is the only acid best known for its ability to dissolve completely silicon carbide, glass materials and other silica based compounds. However, there are biological hazards associated with the use of HF. This is due to its physiochemical properties and its effect on living tissues. Hydrofluoric acid at a concentration of 22 molar has the following properties: it is a non-oxidising acid, with a boiling point of 108 ºC and vapour pressure of 25 bars (at 240 ºC). HF is a clear, colourless liquid; it can be easily mistaken as somewhat harmless. When HF is in contact with the skin, its fluoride ions have the ability to penetrate the skin and damage the tissue and bones (Crouse, 2010). The use of this acid requires significant precautionary measures and extra care.

In our experiments, concentrated nitric acid and sulphuric acid were used along with HF. Nitric acid was used because of its strong oxidising properties and sulphuric acid it also assists in the decomposing the sample because it has a boiling point of about 340 ^{o}C (Sneddon & Butcher, 2002).

Dissolution of silicon carbide was also investigated using ammonium bifluoride ($NH_4F.HF$). This compound is also used to etch silica compounds or as a glass etchant.

7.2.1.1 Dissolution in a Muffle Furnace

The results obtained when attempting to etch samples using a muffle furnace indicated that no layer dissolution took place at all. The particles surface observed after etching did not show any change in the surface. The diameter of the particles also remained the same. As a result of these findings it was decided that no further etching using a muffle furnace should be attempted.

7.2.1.2 Dissolution using a Microwave Heating System

The microwave-assisted reaction system was introduced because of its several advantages; for example reaction time is faster than conventional heating (Coedo et al., 1998). The rapid heating of this system at elevated pressures, assist reactions originating from materials that are difficult to dissolve at low temperatures. This heating technique has previously been used for dissolution of UO_2 fuel particles in a nitric acid media (Zhao & Chen, 2008) and for decomposition of carbide compounds (Coedo et al.,1998).

The microwave system used in the study allows for up to twelve vessels to be employed simultaneously. Of this, one vessel (the control vessel) is used for monitoring temperature and pressure. The control vessel is connected to a fibre optic temperature sensor that penetrates into the vessel and a pressure sensor is attached to the lid. The heating program is controlled and monitored by a microcomputer. It is assumed that the temperature and pressure inside the control vessel is representative of all the samples that are digested simultaneously. However, the volume of the solution that can be used in each vessel is limited to 8 ml.

The closed reaction vessels are designed to reach a maximum temperature of 250 ºC during the heating cycle. The increase of the temperature and pressure in the closed vessels could be a potential safety hazard. Several safety measures are adhered to during the heating process. One is that the set parameters (temperature and pressure)

are monitored using a control vessel. Typical data obtained are shown in Figure 32 and Figure 33, no variation in parameter values is noticeable after heating.

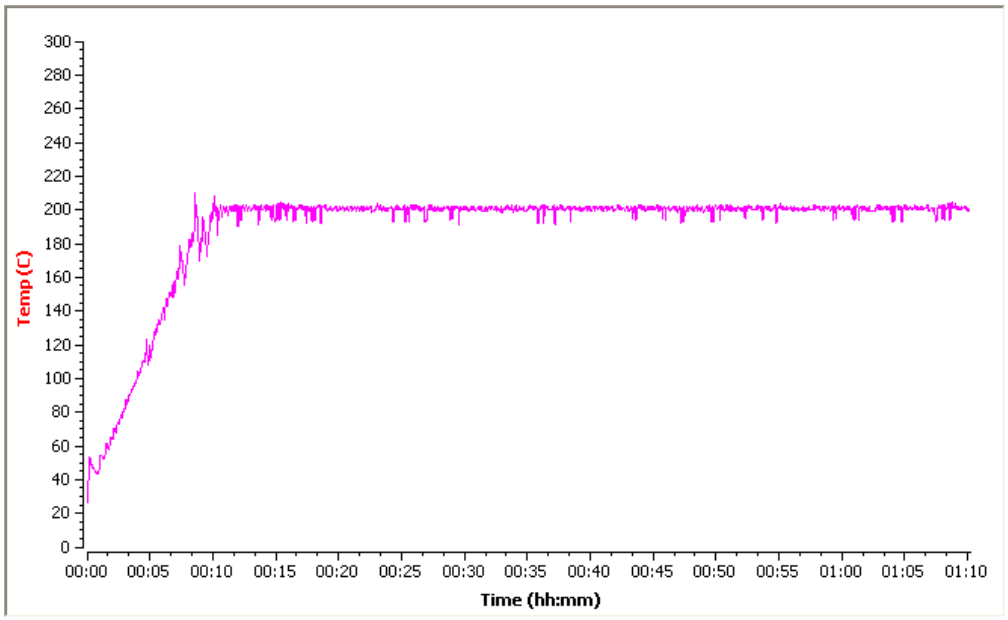

Figure 33:Etching temperature during microwave heating

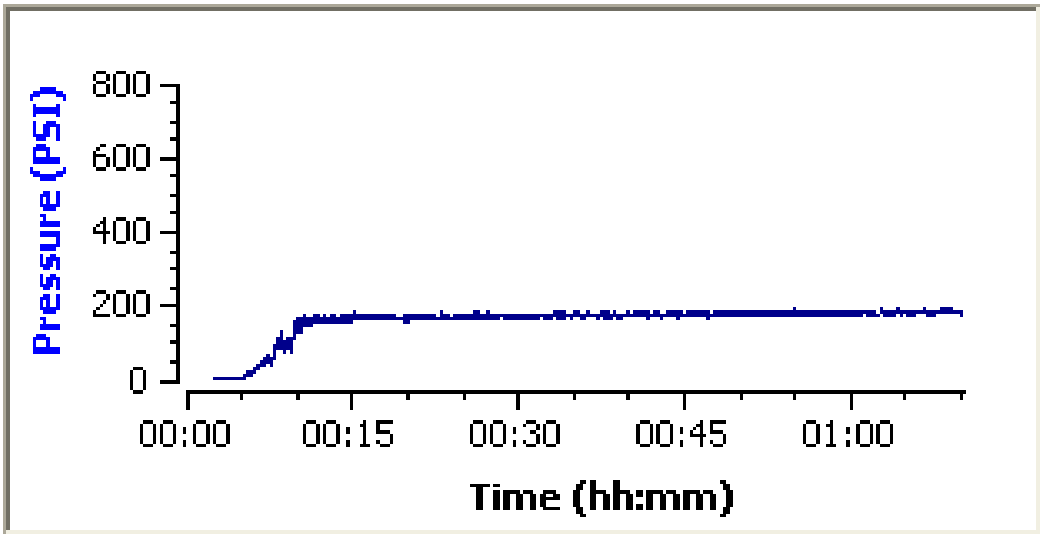

Figure 34 : Pressure generated during microwave heating

7.2.2 Examination of $NH_4F.HF$ and HF Chemically Treated SiC Surface

Treatment with ammonium bifluoride (8 ml at 200 ^{0}C) and with 40 % hydrofluoric acid alone under varying etching conditions (heating temperature 300-350 ^{0}C for about 5 hours) showed no dissolution of the layer. There was no evident decrease in particle diameter during etching and after the etching process.

7.2.3 Examination of $HF/HNO_3/H_2SO_4$ Chemically Treated SiC Surface

7.2.3.1 Optical Microscopy

As mentioned in section 6.6.5 the samples used for silicon carbide etching studies, were particles with virgin SiC surface. The outer surface of these particles visually appeared with similar appearance when compared to particles where the outer pyrolytic carbon layer was removed by etching (optical microscopy image is not attached). The etched surfaces were first investigated by optical microscopy and then with a high resolution ZEISS ULTRA SEM.

Figure 35 displays the optical microscopy images of samples after chemical etching. After 60 minutes of etching Figure 35 (a), the investigation shows the particle surfaces which were observed to have a dull appearance. After etching for 2 hours with $HF/HNO_3/H_2SO_4$ solution under the same conditions, samples were randomly taken from different vessels and examined (Figure 35 (b) and (c)). The results shows that the surface appearing to be yellow coloured grainy structure. In some particles the silicon carbide layer disintegrated into pieces due to the reaction with chemical etchants. Figure 35 (b) shows a black particle, probably the inner pyrolytic carbon layer, where the SiC layer is completely removed, while the other particles do not show any signs of attack. Etching of the layer apparently progresses in an irregular pattern as shown in Figure 35 (c) and results in partial removal of the layer.

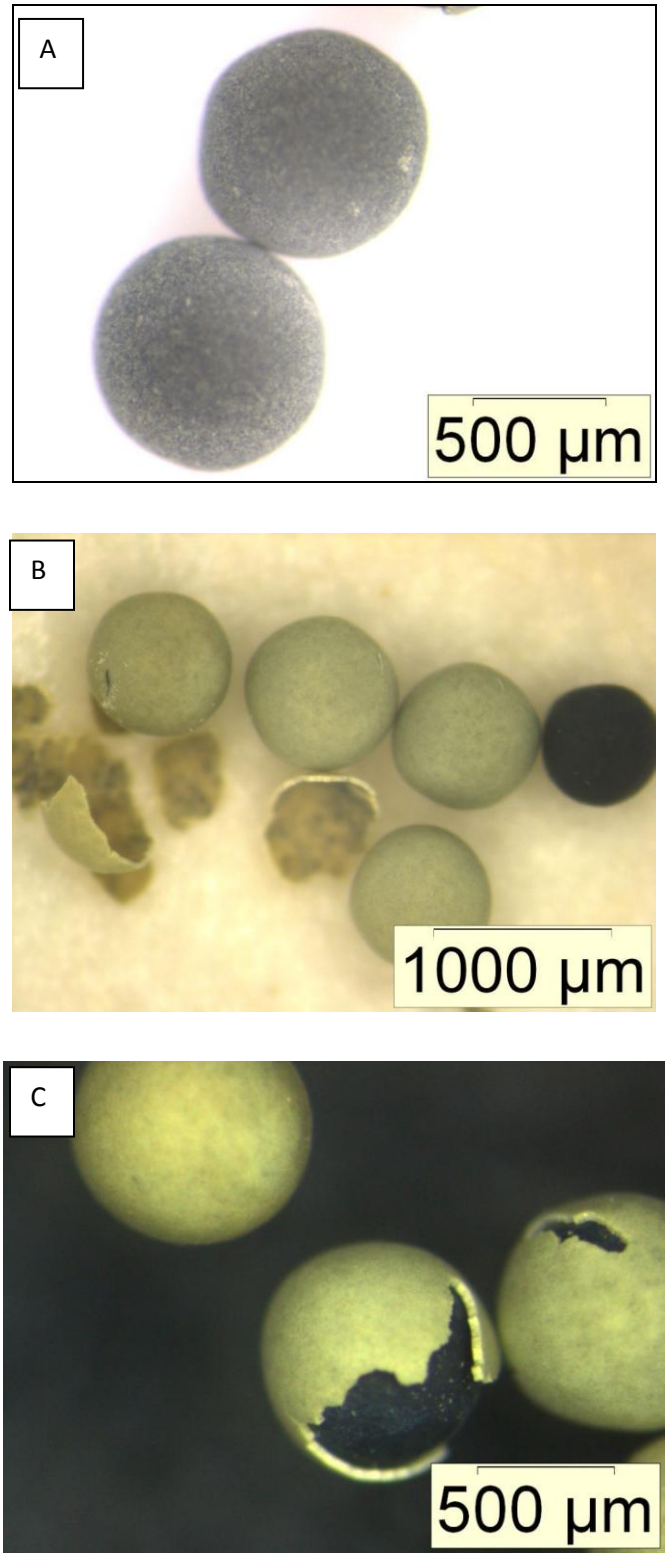

Figure 35: Optical light microscopy images of samples at different stages of chemical treatment (a), (b) and (c)

The broken shells obtained after etching imply that the layer has separated from the rest of the particle. However, the manner in which this layer has been removed is not fully understood. The micro structural characteristics of the black particle (Figure 35 (b)) were investigated with a SEM. The surface consisted of closely packed, smooth globular features (Figure 36). This structure is assumed to be that of the inner pyrolytic carbon layer; however we were unable to compare it to the microstructure of outer pyrolytic carbon layer presented in Figure 27 due to poor contrast. The assumption was therefore made that the silicon carbide layer was completely removed.

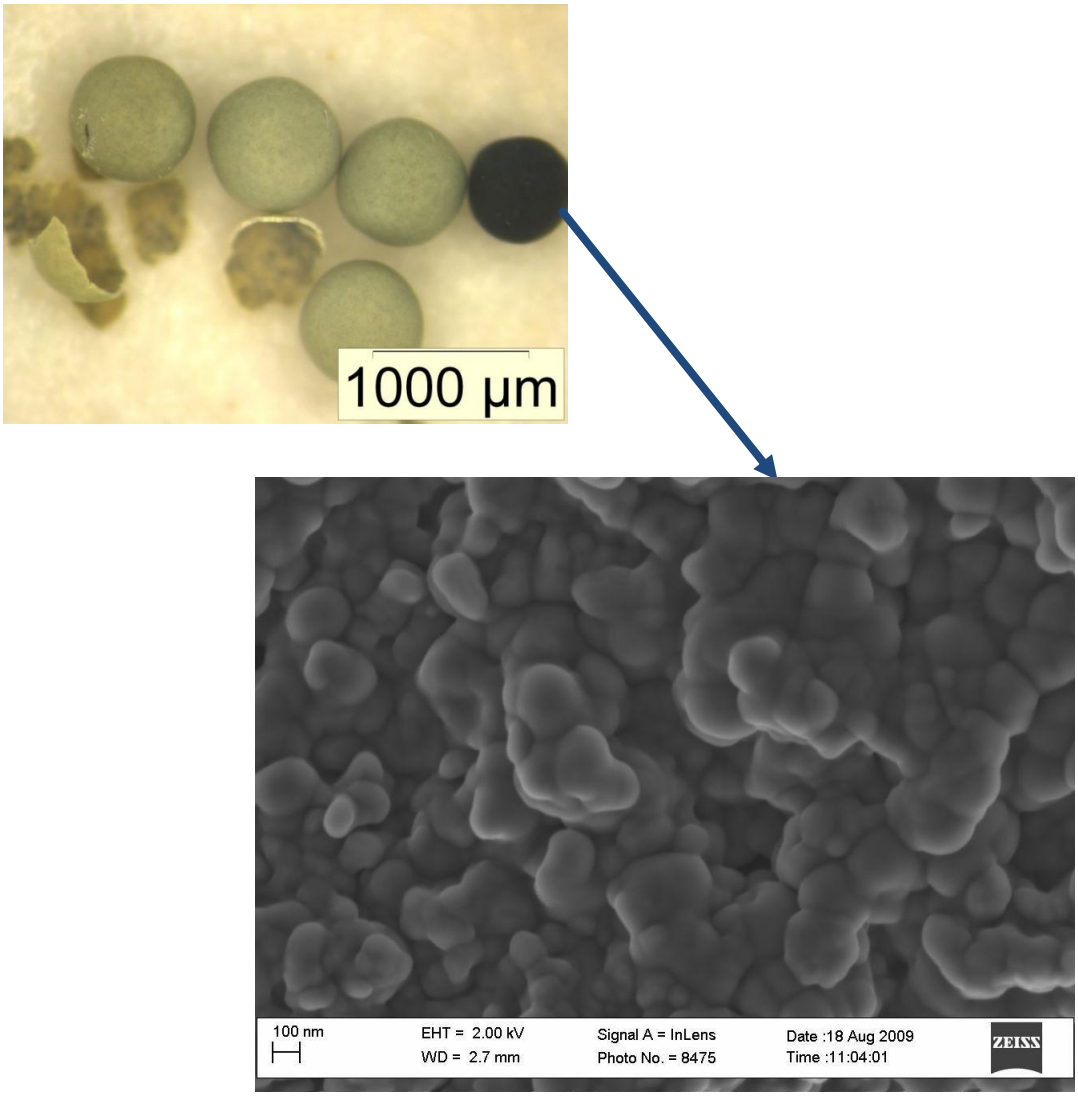

Figure 36: SEM micrograph of the particle with black appearance.

When etching under these experimental conditions, a number of technical problems were encountered: incomplete dissolution of the layer, partial removal and in some cases the layer disintegrated into small pieces. Some particles showed no reaction and the results were not consistent.

7.2.3.2 SEM Examinations

The samples etched in $HF/HNO_3/H_2SO_4$ solution using microwave heating for 1 hour were investigated further using a high resolution SEM. SEM micrographs (Figure 37 (a) and (b)) represent the same region of the sample under investigation but at different magnifications. The etched surface now consists of coarse divided particles. The smooth microstructure observed before etching is now attacked and separated by the etchant.

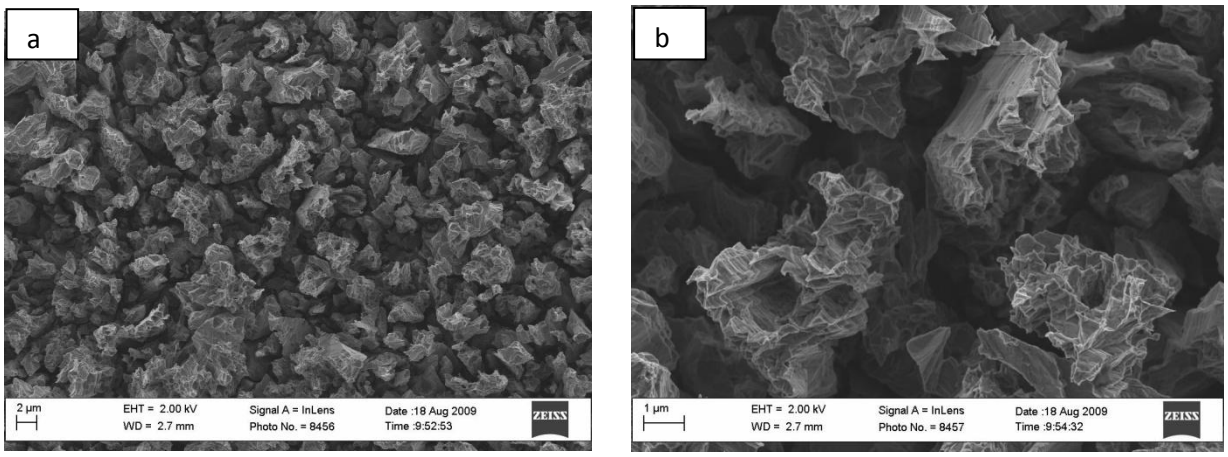

Figure 37: Silicon carbide surface etched for 1 hour in HF/HNO_3-H_2SO_4

The conclusion at this point was that etching under these conditions produces undesirable results. The etching studies using the HF/HNO_3-H_2SO_4 solution were terminated for the reason that partial and non-uniform removal of the layer was observed.

7.2.4 Examination of HF/HNO_3 Chemically Treated SiC Surface

7.2.4.1 Optical Microscopy

Chemical etching with solution number three, a mixture of hydrofluoric acid and nitric acid, produced more or less similar results as the HF/HNO_3-H_2SO_4 solution. Figure 38 represents optical images of samples treated with HF/HNO_3 for 3 hours using the MARS equipment. Partial (Figure 38 (a)) and almost complete (Figure 38 (b)) removal of the SiC layer is apparent in this examination. Furthermore the examination shows that in some particles the silicon carbide layer separated from the rest of the particle leaving an empty shell (Figure 38 (c)). Another sample, obtained from a different vessel (Figure 38 (d)), consist of an intact hollow cracked particle with a slightly orange appearance. This indicates that the coating layers inside were severely attacked by the acid solution and the heating method used. Translucent zirconia kernels were recovered from the solution.

The optical microscopic observations clearly indicate that the etchant and method used offer a possible solution for etching of the silicon carbide layer. A major disadvantage of these experiments is that samples etched under the same conditions show different results.

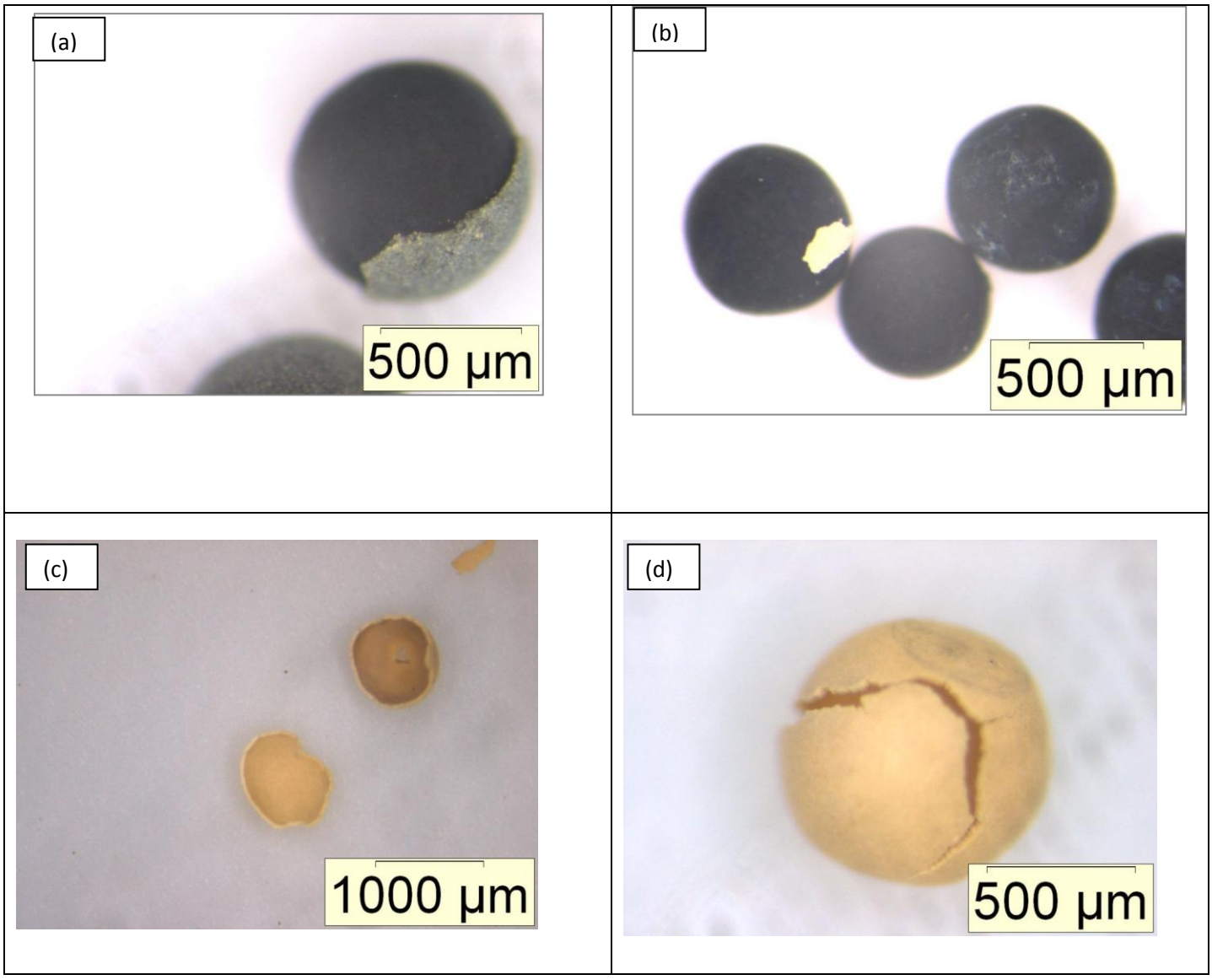

Figure 38: Optical light microscopy images of samples etched in HF/HNO_3 for 3 hours

7.2.4.2 SEM Analysis

SEM micrographs of the sample treated in the microwave system with HF/HNO_3 for 60 minutes at a temperature of 200 ºC are shown Figure 39. The examination Figure 39 (c) shows that the etchant attacks the grains along grain boundaries and to a lesser extent the planar faults that are revealed by somewhat rounded dislocation etch pits. In Figure 39 (d) etching reveals massive degradation of the grain boundaries.

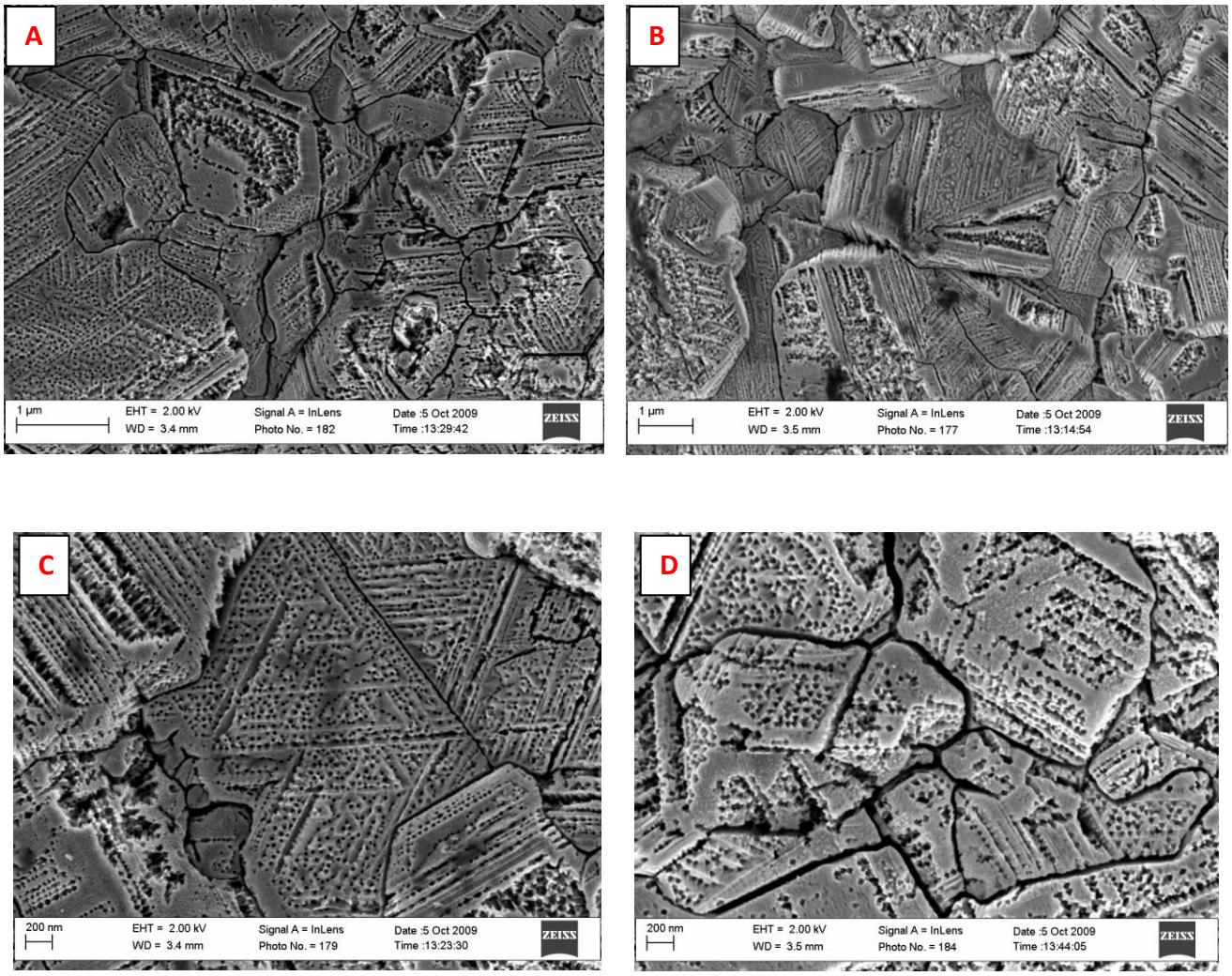

Figure 39: SEM Micrographs of SiC surface etched for 60 minutes

Comparable features (planar faults) on the morphology of an etched SiC surface (Figure 39(c)) were observed by Helary et al. (2008). Their study involved characterization

methods to investigate the microstructures of the coated particle layers prior to irradiation. In their work, Murakami's etchant was used to reveal details of the SiC microstructure. A mounted and polished SiC surface was etched for 60 minutes. Figure 40 adapted from Helary's work, shows crystalline planes with faults at a characteristic angle of about 70º to each other. In Figure 39 (C) the faults revealed by etching were measured and found to be at an angle of about 63º to each other.

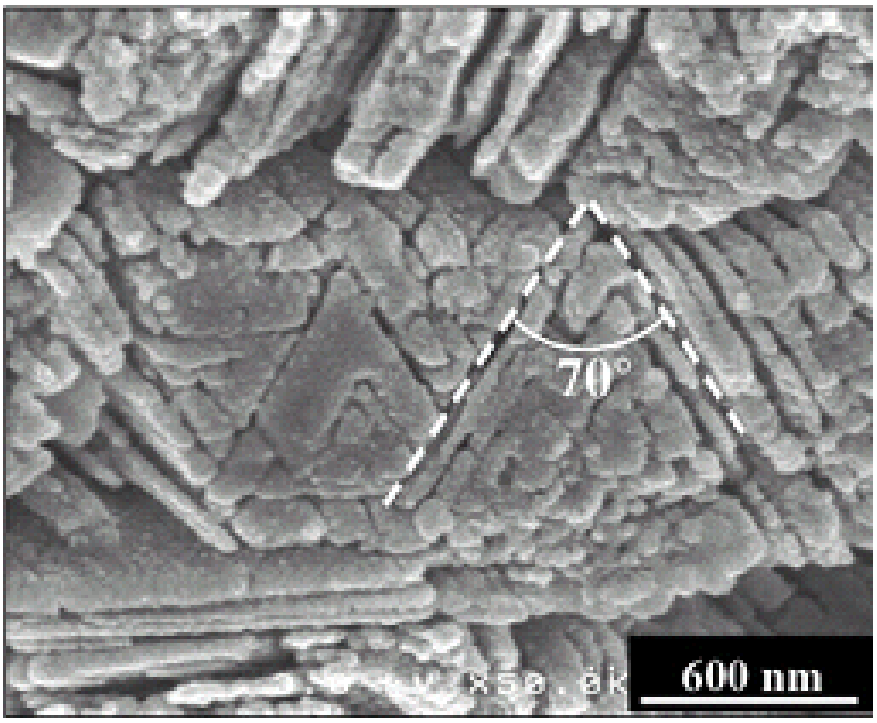

Figure 40: SEM micrograph of polished and etched SiC section reproduced with the permission of the author from Helary et al., (2008).

Figure 41 shows the etched surface of a sample treated under similar conditions as the sample discussed in Figure 39 with the exception of the time that was extended to 2 hours. In this sample the etchant seems to severely attack the grain boundaries thus separating individual grains. The planar faults revealed through etching are again noticeable but a slightly lower magnification was used to clearly indicate the grain separations. The reason for this phenomenon is not fully understood, but it is possible that these effects are due to chemical attack on slip planes (i.e. the displacement planes

along which a crystal deforms under the action of shearing forces) in the silicon carbide crystal.

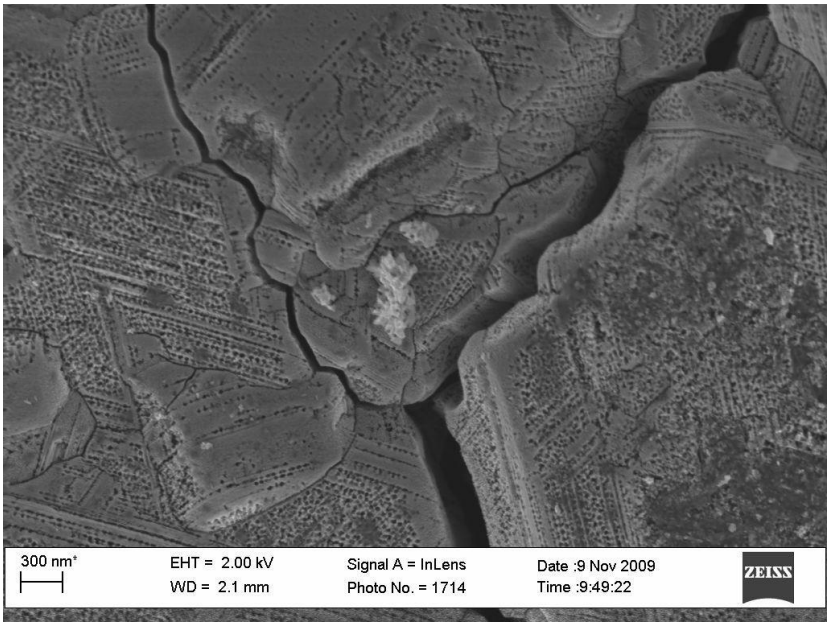

Figure 41: SEM image of particle etched for 2 hours

Higher magnification Figure 42 shows severely etched slip planes consisting of jagged contours.

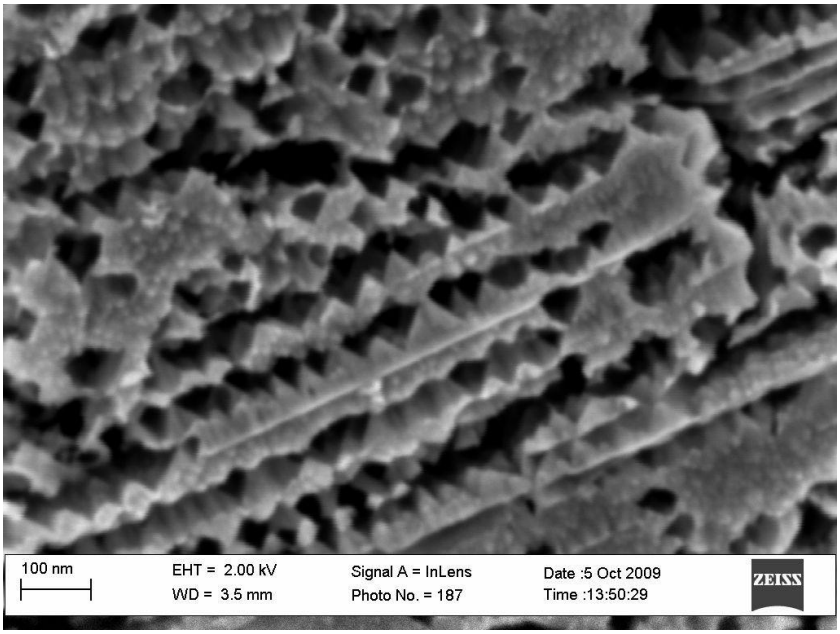

Figure 42: SEM micrograph of SiC structure after 2 hours

At prolonged time, 3 hours of etching at 200 ºC (Figure 43); the etched sample disintegrates into single crystals with needle like appearance and maximum size of 8 µm.

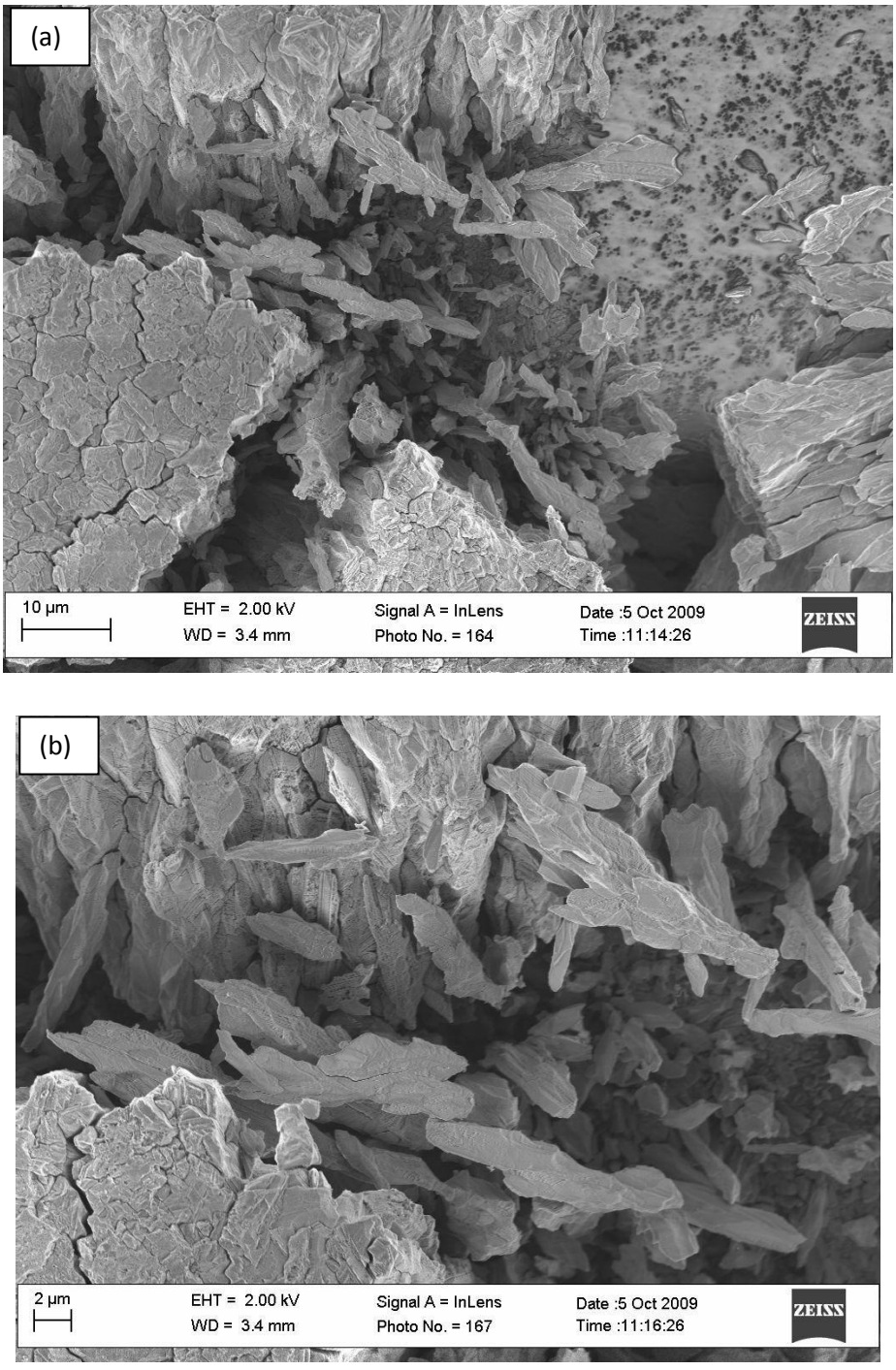

Figure 43: SEM micrograph of SiC structure after 3 hours

7.2.4.3 X-ray Diffraction (XRD) Analysis

The samples used for XRD analysis to determine phase composition were the original (with outer layer silicon carbide) and the coated particles that were treated with HF\HNO_3 under microwave heating for 3 hours. The latter samples consisted of silicon carbide shells obtained after treatment where inner carbon coatings were dissolved (Figure 38 (C)). Experimental parameters measured with Cu kα radiation at wavelength of 1.5406 angstrom are presented in Table 10.

Table 10: XRD-measured parameters

Measurement	Parameter
Diffractometer	D8 Advance
Goniometer	θ-θ
Recording range	20˚ to 130˚
Frame width	0.04˚
Counts/frame	0.4s

Figure 44, shows diffraction patterns of the original sample surface (black) and samples after chemical treatment (red). The two patterns show similarity in terms of peak position. The differences observed in peak intensity can be attributed to variations in sample volume probed. The broad humps at low angles (from 20 to 36°) indicate that the samples are not partly amorphous.

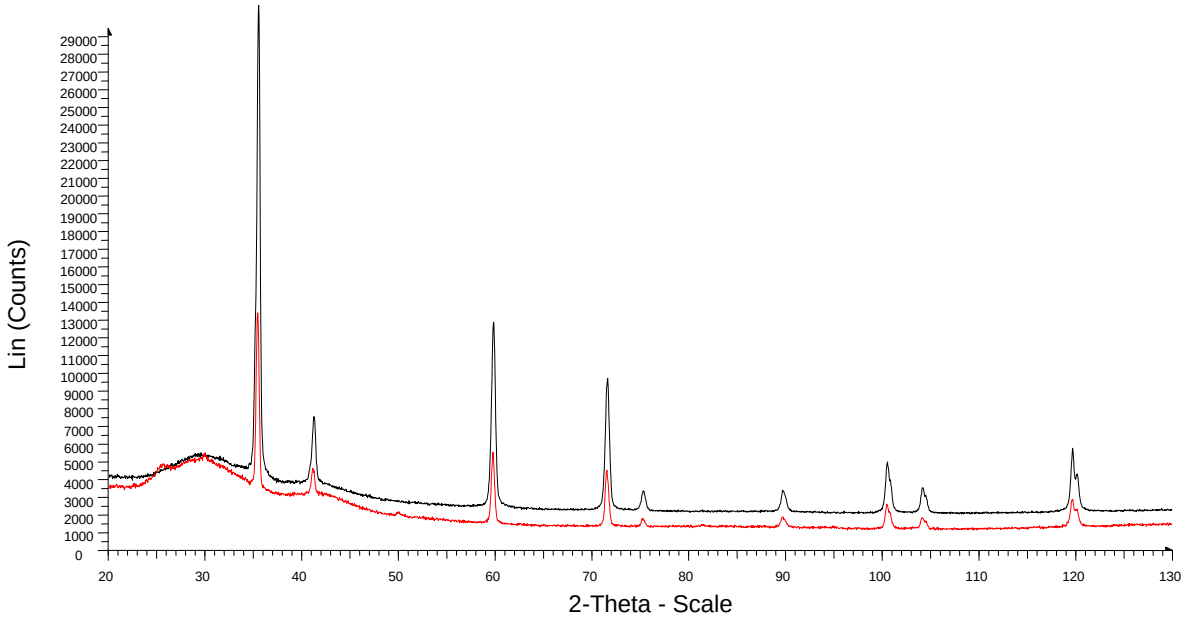

Figure 44: X-ray–Diffraction pattern on etched (red) and unetched (black) SiC sample

Figure 45 demonstrates the superposed powder diffraction pattern of original samples and etched ones overlaid with stick patterns of the proposed crystalline phases (Moissanite; 3C-SiC). In this analysis the background and Kα2 are subtracted for identification of the pattern, hence the broad humps seen in spectra of Figure 44 are not visible in Figure 45.The pattern shows that the samples are predominantly silicon carbide. However peaks observed at approximately 25, 30 and 50º in 2θ in the etched samples correspond to minor carbon phase.

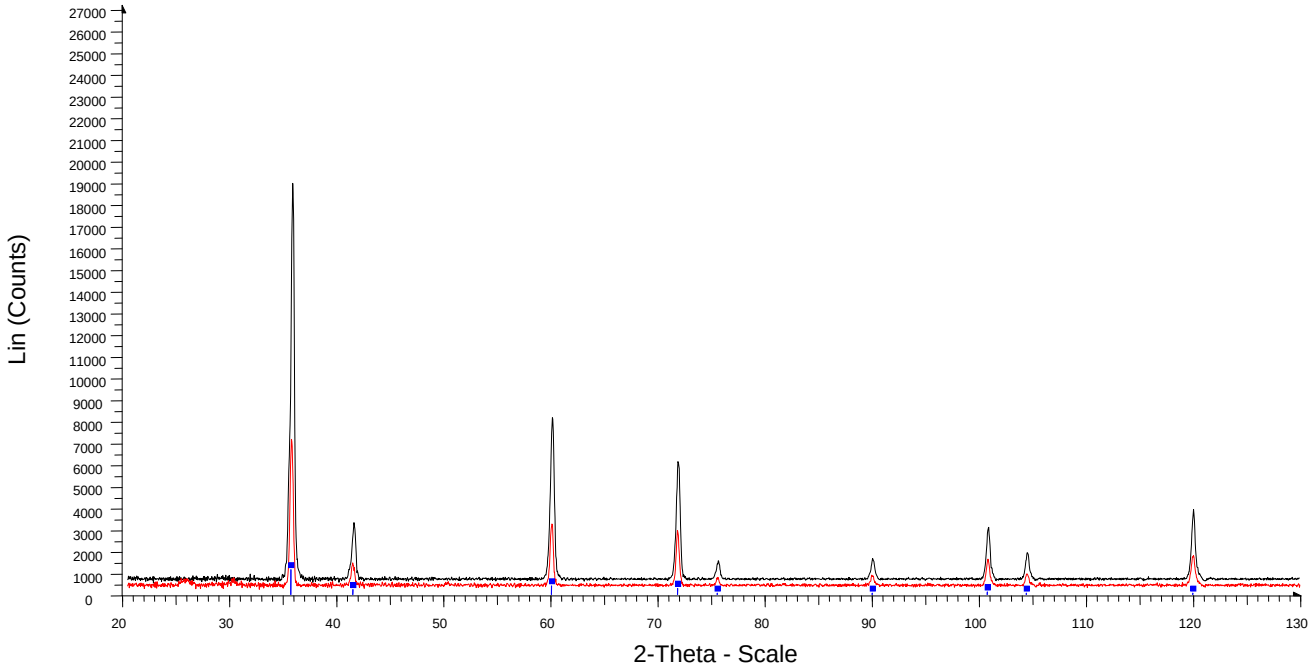

Figure 45: XRD pattern of unetched samples (black) and etched (red) ones overlaid with stick patterns of the proposed crystalline phases.

The XRD analysis shows that both samples are mainly silicon carbide with a minority carbon phase in the chemically treated sample. Comparing the two X-ray diffraction patterns Figure 44 and Figure 45, there is no obvious difference in the peak position. It is likely that the silicon carbide samples pieces obtained after etching have a similar crystalline structure as unetched silicon carbide samples. This analysis was not investigated in detail; the amount of the sample was not enough for analysis.

CHAPTER 8

SUMMARY

This study was undertaken to investigate a simple reliable wet chemical etching procedure for layer-by-layer etching of TRISO particle layers. The possibility of this method to etch the particle layers in a controlled manner was evaluated to determine if each layer can be dissolved separately and later on apply the method for irradiated fuel to trace the release and distribution of fission products from the kernel and layers. Due to chemical inertness of the particle layers dissolution experiments were conducted using vigorous acids such as nitric acid, sulphuric acid, perchloric acid and hydrofluoric acid.

The surface of the particles before and after etching was studied first by light microscopy and then by scanning electron microscopy. Energy dispersive X-ray analysis was used to identify elemental surface composition before and after chemical etching of the outer pyrolytic carbon layer. X-ray diffraction was employed to study the phase identification of the silicon carbide pieces resulting from etching samples and unetched silicon carbide samples.

The etching investigations were limited to two outermost coatings: outer pyrolytic carbon and silicon carbide. Due to difficulties experienced in etching the silicon carbide layer, we were unable to proceed to the underlying carbon layers. Also due to the closure of the PBMR project we were unable to proceed with further the investigations

8.1 ETCHING OF OUTER PYROLYTIC CARBON LAYER

Two heating methods, heating using a hot plate and using a reflux system, were explored to investigate dissolution of the OPyC layer. The use of reflux system for heating seems to have a positive influence in the etching process. The system allowed the reaction to be heated at temperatures of 130 ºC for a long time without changing the

acid solution. Etching using the hot plate was found to have some limitations, with the solution evaporating when heated to temperatures between 120 to 130 ºC.

The experimental results show that the outer pyrolytic carbon layer can be readily removed with the use of strong oxidising acids composed of concentrated nitric acid, sulphuric acid mixed with chromium trioxide acid. The temperature for effective removal of this coating was found to be in range of 120 to 130 ºC for etching of single coated particle. The favourable experimental conditions for removal of OPyC from a single coated fuel particle were identified and found to depend on etching solution, etching time and etching temperature.

SEM analyses demonstrated that the outer carbon material was removed completely. The surface revealed by SEM was identified to be of silicon carbide by EDS analysis. In the EDS results it was shown that the removal of the layer was not affected by acid solutions as the analysis did not show any chemical species from the etchants.

Based on these findings it can be concluded that chemical etching of the outer pyrolytic carbon layer gives uniform and complete removal using a solution of $HNO_3/H_2SO_4/CrO_3$ at temperatures of 130 to 140 ºC leaving the exposed silicon carbide layer.

8.2 ETCHING OF SILICON CARBIDE LAYER

Etching of the silicon carbide with conventional heating was found to be ineffective. Microwave assisted chemical etching was the only heating technique found to be useful. The advantages of the microwave heating include, fast reaction times and small amounts of acid solution required. The use of common chemical etchants has been found to be ineffective for dissolving this layer. In the initial experiments only fluoride containing substances showed the potential to etch the layer. The experimental results show that a mixture consisting of equal amounts of concentrated hydrofluoric and nitric acid under microwave heating at 200 ºC yielded partial removal of the coating and localized attack of the underlying coating layers

The SEM analyses yield the morphology of the surface samples before and after different stages of the etching step.

The manner in which the silicon carbide dissolved is not well understood at this point. The etching results using etchants yielded partial removal of the coating in some samples. The etching is observed to proceed predominantly along intergranular and intragranular routes.

Etching of SiC has been found to have shortcomings such as undesired dissolution of the inner carbon layers and cracking of the sample. Etching of the silicon carbide layer in a HF media under microwave digestion results in a poorly selective etch, that does not provide uniform and complete removal. The etchant behaviour for $HF/HN0_3$ and $HF\text{-}HNO_3\text{-}H_2SO_4$ seems vastly different comparing figure 34-42 yet the only difference is the exclusion of sulphuric acid. It could be useful to study extensively the kinetics of the dissolution with and without sulphuric acid using the same parameters described in Chapter 7.

This study was terminated due to the collapse of the PBMR project. We were unable to continue with the experimental studies. At the time of writing, it was not easy to evaluate and conclude that the wet chemical etching methods can be applied to irradiated fuel. Additional oxidation options to investigate would have been molten salts, e.g. peroxides or carbonate/hydroxide/nitrate mixtures. However, the higher operation temperatures would have made these less attractive.

REFERENCES

Ablitzer, C. C. (2007). CVD in fluidized-bed furnace pyrolytic carbon and SiC deposition. *Eurocourse on Coated Particle Fuel, EC-Raphael Puma.* NRG, Petten, The Netherlands.

Baker, D. (1971). Graphite as a Neutron Moderator and Reflector Material. *Nuclear Engineering and Design* , 413-444.

Barry, J. (2008, April). Manufacture of TRISO coated particles. *Personal Communication* .

Batchelor, A. L. (2002). *Materials Degradation and its Control by Surface Engineering.* London: Imperial College Press.

Betz, G. D. (1971). Determination of the distribution of fission products in fuel particle coatings by the sputtering technique. *Journal of Nuclear Materials , 38*, 77-79.

Bhat, S. (2002). *Biomaterials.* India: Kluwer Academic Publishers.

Boehm, E. (1994). Nomenclature and terminology of graphite interacalation compounds. *Pure and Applied Chemistry , 66* (9), 1893.

Botha, A. (2009, October). Technical Report: Scanning electron microscope analysis on TRISO particles. *Scanning electron microscope analysis on TRISO particles* . South Africa.

Brink, D. M. (2009). Neutron irradiation effects in SiC. *Nuclear Instruments and Methods in Physics Research , 267*, 2716-2718.

Bokros, J. (1969). *Chemistry and Physics of Carbon.* New York: Marcel Dekker.

Burchell, T. a. (2007). The effect of neutron irradiation damage on the properties of grade NBG-10 graphite. *Journal of Nuclear Materials , 371*, 18-21.

Burchell, T. (2001). Thermal and Nuclear Energy Applications. In P. Delhaes, *Graphite and Precursors* (p. 94). Netherlands: Gordon & Breach Science Publishers.

Buzelli, G. a. (1977). Percholric acid dissolution of graphite and pyrolytic carbon. *Talanta , 24*, 383- 384.

Camba, G. Y. (2006). Anisotropic etching of SiC whiskers. *American Chemical Society , 6*, 548-550.

Carter, R. a. (1955). Proceedings of the Conferences on Carbon -Moderator Graphite for High Temperature Reactor. *Nuclear Engineering and Manufacturing* .

Choi, W. a.-T. (1998). Nitric acid uptake and decomposition on black carbon (soot) surfaces: Its implications for the troposphere and lower stratosphere. *J.Phys.Chem , 102*, 7618-7621.

Chung, D. (1994). *Carbon Fiber Composites.* Washington: Butterworth-Heinemann.

Chunhe, T. X. (September 22 -24, 2004). The behaviour of HTR-10 fuel under irradiation. *Proceedings of the 2nd International topic meeting on High Temperature Reactor Technology (2004).* Beijing, China.

Coedo, A. D. (1998). Study of the parameters in microwave dissolution methods using a magnetic stirring device in the microwave unit: application to dissolution of high carbon ferrochromium. *Analyst , 123*, 1209-1212.

Coedo, A. D. (1998). Use of boric acid to improve the microwave-assisted dissolution process to determine flouride elements in steels by flow injection inductively coupled plasma mass spectrometry. *Journal of Analytical Spectrometry , 13*, 1193.

Cotton, A. a. (1980). *Advanced Inorganic Chemistry- A Comprehensive Guide.* New York: John Wiley and Sons.

Crouse, P. (2010). Safe handling of hydrogen flouride. University of Pretoria.

Cullity, B. (1977). *Elements of X-ray Diffraction.* Boston: Addison-Wesley.

Dauskardt, R. a. (1993). Pyrolytic Carbon Coatings. In L. a. Hench, *An Introduction to Bioceramics* (pp. 261-272). Singapore: World Scientific Publishing Co. Pte. Ltd.

DelCul, G. S. (September, 2002). *TRISO coated fuel processing to support high temperature gas cooled reactors.* Tennessee: Oak Ridge National Laboratory.

Fukuda, K. a. (1977). Concentration profiles of fission products in the coating layers of irradiated fuel particles. *Journal of Nuclear Materials , 66*, 55-58.

Fukuda, K. a. (1976). Determination of the fission product distribution in SiC coating layer of fuel particles. *Mikrochimica Acta , II*, 99-105.

Fukuda, K. a. (1975). Diffusion and evaporation of fission products in coated fuel particles. *Journal of Nuclear Science and Technology , 12*, 181-182.

Gabouze, N. K. (2009). Chemical etching investigation of polycrystalline P-type 6H-SiC in HF\Na2O2 solutions. *Applied Surface Science , 255*, 6751.

Grambow, B. A. (2006). Study of various options for final disposal of HTR coated particles. *Proceedings of the 3rd International Topical Meeting on High Temperature Reactor Technology (HTR 2006).* Johannesburg, South Africa.

Gulol, O. C. (2008). Performance analysis of TRISO coated fuel partiles with kernel migration. *Journal of Nuclear Materials , 374*, 168-173.

Habuka, H. O. (2006). Etching in chlorine gas. *Thin Solid Films , 514*, 193-194.

Harris, G. (1995). *Properties of Silicon Carbide.* United Kingdom: INSPEC.

Helary, D. D. (2008). Advanced characterization techniques for SiC and PyC coatings on high temperature reactor fuel particles. *Journal of Nuclear Materials , 373*, 150-154.

Hunter, S. I. (1990). *Methods employed in the analysis of components from high temeprature reactor graphite fuel elements.* Technical Report- Unpublished document.

IAEA. (1997). Fuel performance and fission product behaviour in gas-cooled reactors. *IAEA-TECDOC-978* . International Atomic Energy Association.

Inamati, S. R. (1985). *Gaseous and metallic fission product transport characteristics of a modular pebble bed HTGR during loss of core cooling accidents.* Retrieved October 20, 2009, from IAEA, Vienna: www.iaea.org/inisnkm/aws/htgr/abstract/abst.17036728

Jones, A. a. (2010). Nuclear Graphite Manufacture, Microstructure and Virgin Properties. *Carbowaste.* Abbeys St Jacus.

Kendall, J. a. (2004). Advanced coated particle fuel options. *The proceedings: 2nd International Topical Meeting on High Temperature Reactor Technology.* Beijing, China.

Kercher, A. H. (2008). Automated optical microscopy of coated particle fuel. *Journal of Nuclear Materials , 380*, 77.

Kim, J. K. (2007). Study of CVD SiC deposition for TRISO coated fuel material fabrication by computational simulation and actual experiment. *Journal of Ceramic Processing Research , 8*, 389-390.

Kim, W. P. (2009). Effect of coating temperature on properties of the SiC layer in TRISO coated particles. *Journal of Nuclear Materials , 392*, 213-216.

Kimoto, T. a. (2004). Epitaxial growth of high quality silicon carbide- Fundamentals and recent progress. In Z. a. Feng, *Materials, Processing and Devices* (pp. 1-10). New York: Taylor & Francis book, Inc.

Klopper, W. (S.A, July 2010). The guidebook post irradiation examination of HTR fuel elements. Pretoria, South Africa: Personal Communication.

Landolt, H. M. (1984). Device Technology. In *Numerical data and functional relationship in science and technology.* New York: Springer.

Languille, A. (2002). HTR coated particles and fuel elements. *Conference on High Temperature Reactors, HTR 2002.* Petten.

Lopez-Honorato, E. M. (2009). Fluidized bed chemical vapour deposition of pyrolytic carbon - effect of deposition conditions on microstructure. *Carbon , 47*, 396-398.

Markgraaff, J. (2009). High Temperature Reactor Fuel Materials. *Course Notes* . University of North West, Potchefstroom Campus.

Marsden, B. F. (2005). Irradiation behaviour and structural analysis of HTR/VHTR graphite core components. *18th International Conference on Structural Mechanics in Reactor Technology.* Beijing, China.

Miller, G. P. (2004). Consideration of the effects of partial debonding of the IPyC and particle asphericity on TRISO-coated feul behaviour. *Journal of Nuclear Materials , 334*, 79-81.

Minato, k. O. (2000). Retention of fission product caesium in ZrC coated fuel particles for high temperature gas cooled reactors. *Journal of Nuclear Materials , 279*, 181.

More, R. H. (2004). Pyrolytic Carbon for Long-Term Implants. In B. Ratner, *An Introduction to Materials in Medicine* (pp. 170-172). USA: Eslvier Academic.

Nabielek, H. S. (1989). The performance of high-temperature reactor fuel particles at extreme temperature. *Journal of Nuclear Technology , 84*, 62-78.

Nabielek, H. v.-T. (2009). Ceramics coated particles for safe operation in HTRs and in long term storage. In Y. a. Katoh, *Ceramics in Nuclear Applications: Ceramic Engineers and Science Proceedings* (pp. 193-202). Canada: John Wiley & Sons, Inc.

Park, J. a. (2007). *Biomaterials an Introduction.* USA: Springer Science.

Pearton, S. (2006). Dry etching of SiC. In R. Cheung, *Silicon Carbide Micro Electromechanical Sytems for Harsh Environments* (p. 103). London: Imperial College Press.

Petti, D. a. (2002). Coated Particle fuel behaviour under irradiation. *Coated Particle Fuel Behaviour under Irradiation Euro-Course.* France.

Petti, D. (2006). Fuel Failure Mechanisms. *HTR Fact Book* . Unpublished document.

Pierson, H. (1993). *Handbook of Carbon,Graphite,Diamond and Fullerenes.* United States: Noyes Publication .

Pierson, H. (1999). *Handbook of Chemical Vapor Deposition: Principles, Technology and Application.* New York: Noyes Publication.

Rand, B. (2009, August). Carbon Materials Science. *Course Notes* . Pretoria: University of Pretoria.

Reimer, L. (1998). *Scanning Electron Microscopy Physics of Image Formation and Microanalysis.* New York: Springer.

Reitsamer, G. P. (S.A). *Google*. Retrieved June 10, 2009, from http://www.iaea.org/htgr

Ruggirello, G. a. (2006). Modelling of V/HTR fuel elements and coated particles; needs of post irradiation examination in support to the European" Raphael" and GEN-IV Projects. *IAEA Technical Meeting on Hot Cell Post Irradiation Examination Techniques and Poolside inspection of Water Reactor Fuel Assemblies.* Buenos Aires.

Saddow, S. a. (2004). *Advances in Silicon Carbide Processing and Applications.* London: Artech House,Inc.

Sharma, B. (1995). *Nuclear and Radiation Chemistry.* Meerut: Krishma Prakashan Media (P) Ltd.

Shenoy, A. a. (2009). High Temperature Gas Cooled Reactors. In K. Kok, *Nuclear Engineering Hand Book* (pp. 203-204). Boca Raton: CRC Press.

Snead, L. N. (2007). Handbook of SiC properties for fuel performance modeling. *Journal of Nuclear Materials , 371*, 329-351.

Sneddon, J. a. (2002). *Advances in Atomic Spectroscopy* , 376-378.

Somiya, S. a. (1988). *Silicon Carbide Ceramics- Fundamental and Solid Reaction.* New York: Elsevier.

Sone, H. K. (2000). In situ measurements and growth kinetics of silicon carbide chemical vapour deposition from methlytrichlorosilane. *Journal of Crystal Growth , 219*, 245.

van Dorp, D. W. (2007). Anodic etching of SiC in an alkaline solution. *Journal of micromechanics and microengineering , 17*, 50.

Verfondern, K. N. (2007). Coated particle fuel for high temperature gas cooled reactors. *Nuclear Engineering and Technology , 39*, 603.

Verfondern, K. S. (1990). Passive safety characteristics of fuel for a modular high temperature reactor and fuel performance modeling under accident conditions. *Journal of Nuclear Technology , 91*, 235-240.

Wickham, A. a. (2004). The IAEA international database on irradiated nuclear graphite properties, A sucess story for both new build and life extension of commercial power plants . *The IAEA international database on irradiated nuclear graphite properties* . IAEA.

Xu, S. Z. (1995). Effects of deposition temperature on the properties of pyrolytic silicon carbide. *Journal of Nuclear Materials , 224*, 12.

Yamada, Y. a. (1998). Properties and applications of silicon carbide. In S. a. Somiya, *Silicon Carbide Ceramic- Fundamental & Solid reactions* (pp. 12-16). New York: Elsevier.

Yan, W. K. (2004). Graphite intercalation chemistry with large flouroanions. *Journal of Flourine Chemistry , 125*, 1703.

Zappe, S. (2006). Properties of Silicon Carbide. In R. Cheung, *Introduction to Silicon Carbide micro electromechanical system for harsh environments* (p. 130). London: Imperial College Press.

Zhao, Y. a. (2008). Studies on the dissolution kinetics of ceramic uranium dioxide particles in nitric acid by microwave heating. *Journal of Nuclear Materials , 373*, 53-54.

Zinovev, A. M. (2006). Etching of hexagonal SiC surfaces in chlorine-containing gas media at ambient pressure. *Surface Science , 600*, 2242-2251.

APPENDICES

Appendix A: Diameter measurements before etching of the OPyC layer

Particle No	Particle diameter measurements (mm)						Mean per particle (mm)
Particle #1	0.98	0.97	0.99	0.97	0.99	0.98	**0.98**
Particle # 2	0.96	0.97	0.96	0.95	0.96	0.95	**0.96**
Particle #3	0.99	0.98	0.99	0.98	0.99	0.99	**0.99**
Particle #4	0.98	0.99	0.96	0.98	0.99	0.97	**0.98**
Particle #5	0.95	0.96	0.96	0.95	0.96	0.96	**0.96**
Particle #6	0.96	0.97	0.97	0.97	0.97	0.97	**0.97**
Particle #7	0.98	0.97	0.97	0.97	0.98	0.99	**0.98**
Particle #8	0.99	0.98	0.97	0.98	0.96	0.96	**0.97**
Particle #9	0.99	0.98	0.99	0.98	0.97	0.99	**0.98**
Particle #10	0.95	0.95	0.96	0.94	0.95	0.96	**0.95**
Particle #11	0.98	0.98	0.99	0.98	0.98	0.97	**0.98**
Particle #12	0.97	0.96	0.95	0.97	0.95	0.97	**0.96**
Particle #13	0.94	0.94	0.96	0.94	0.97	0.96	**0.95**
Particle #14	0.96	0.95	0.95	0.97	0.97	0.97	**0.96**
Particle #15	0.98	0.97	0.97	0.98	0.97	0.96	**0.97**
Particle #16	0.97	0.98	0.98	0.97	0.96	0.98	**0.97**
Particle #17	0.99	0.98	0.99	0.99	0.97	0.99	**0.99**
Particle #18	0.98	0.99	0.99	0.97	0.99	0.98	**0.98**
Particle #19	0.97	0.96	0.95	0.96	0.95	0.96	**0.96**
Particle #20	0.96	0.97	0.97	0.96	0.96	0.97	**0.97**
Particle #21	0.97	0.99	0.99	0.97	0.98	0.96	**0.98**
Particle #22	0.94	0.96	0.96	0.94	0.96	0.95	**0.95**
Particle #23	0.98	0.99	0.97	0.96	0.98	0.97	**0.98**
Particle #24	0.96	0.96	0.95	0.97	0.96	0.97	**0.96**
Particle #25	0.96	0.95	0.96	0.95	0.98	0.96	**0.96**
Particle #26	0.98	0.96	0.98	0.98	0.96	0.97	**0.97**
Particle #27	0.97	0.97	0.96	0.97	0.96	0.95	**0.96**
Particle #28	0.95	0.97	0.97	0.98	0.98	0.98	**0.97**
Particle #29	0.95	0.97	0.95	0.97	0.98	0.97	**0.97**
Particle #30	0.98	0.95	0.98	0.96	0.99	0.97	**0.97**
Mean diameter (all measurements):							**0.97**
Standard deviation (all measurements):							**± 0.01**

Appendix B: Diameter measurements after etching of the OPyC layer

Particle No	Particle diameter measurements (mm)							Mean per particle (mm)
CP #1	0.86	0.86	0.87	0.87	0.87	0.87	0.87	0.87
CP #2	0.88	0.88	0.87	0.87	0.88	0.88	0.86	0.87
CP #3	0.87	0.88	0.88	0.86	0.87	0.86	0.87	0.87
CP #4	0.84	0.85	0.86	0.84	0.86	0.86	0.85	0.85
CP #5	0.87	0.86	0.87	0.86	0.88	0.86	0.86	0.87
CP #6	0.87	0.85	0.84	0.86	0.85	0.85	0.86	0.85
CP #7	0.86	0.86	0.85	0.85	0.84	0.85	0.85	0.85
CP #8	0.86	0.86	0.85	0.87	0.86	0.87	0.86	0.86
CP #9	0.84	0.84	0.85	0.84	0.86	0.85	0.85	0.85
CP #10	0.87	0.86	0.87	0.87	0.86	0.86	0.87	0.87
CP #11	0.89	0.89	0.88	0.89	0.87	0.87	0.87	0.88
CP #12	0.84	0.86	0.84	0.84	0.85	0.86	0.86	0.85
CP #13	0.85	0.86	0.87	0.86	0.87	0.87	0.87	0.86
CP #14	0.9	0.87	0.89	0.87	0.88	0.9	0.89	0.89
CP #15	0.86	0.87	0.88	0.87	0.86	0.86	0.87	0.87
CP #16	0.84	0.84	0.85	0.86	0.85	0.85	0.86	0.85
CP #17	0.89	0.88	0.9	0.88	0.9	0.88	0.89	0.89
CP #18	0.84	0.85	0.86	0.85	0.86	0.84	0.86	0.85
CP #19	0.87	0.87	0.85	0.86	0.85	0.86	0.85	0.86
CP #20	0.86	0.84	0.85	0.86	0.85	0.87	0.86	0.86
CP #21	0.84	0.85	0.84	0.86	0.85	0.85	0.85	0.85
CP #22	0.86	0.86	0.85	0.85	0.86	0.86	0.85	0.86
CP #23	0.87	0.88	0.87	0.86	0.86	0.87	0.88	0.87
CP #24	0.9	0.89	0.89	0.9	0.89	0.88	0.88	0.89
CP #25	0.86	0.86	0.87	0.88	0.87	0.88	0.89	0.87
CP #26	0.89	0.9	0.89	0.9	0.9	0.88	0.89	0.89
CP #27	0.87	0.88	0.87	0.86	0.88	0.87	0.87	0.87
CP #28	0.86	0.87	0.85	0.86	0.87	0.86	0.85	0.86
CP #29	0.89	0.88	0.9	0.9	0.9	0.88	0.89	0.89
CP #30	0.84	0.85	0.85	0.86	0.84	0.86	0.85	0.85
Mean diameter (all measurements) :								**0.87**
Standard deviation (all measurements):								**± 0.02**